INSTITUTE
for
FLUID DYNAMICS
and
APPLIED MATHEMATICS

Technical Note BN-718 November 1971

ONE DIMENSIONAL LUNAR ASH FLOW WITH AND WITHOUT HEAT TRANSFER

by

S.I. Pai and T. Hsieh

UNIVERSITY OF MARYLAND
College Park

Technical Note BN-718 November 1971

ONE DIMENSIONAL LUNAR ASH FLOW WITH AND WITHOUT HEAT TRANSFER

by

S.I. Pai and T. Hsieh

Institute for Fluid Dynamics and Applied Mathematics

University of Maryland

College Park, Maryland

20742

This research was supported in part by the National Aeronautics and Space Administration under NASA Grants No. NGR 21-002-256 and No. NGR 21-002-296. The computer time for this report was supported by NASA Grant NSG-398 to the Computer Science Center of the University of Maryland

Table of Contents

ABSTRACT

The one dimensional steady ash flow has been studied by the two phase flow theory of a mixture of a gas and small solid particles, with special emphasis on the lunar ash flow. For the general ash flow with heat transfer, we have to consider seven variables: the pressure of the mixture p, the temperature of the gas $T_g = T$, the temperature of the solid particles T_p, the velocity of the gas u_g, the velocity of the solid particles u_p, the species density of the gas ρ_g and the volume fraction Z of the solid particles. The fundamental equations and boundary conditions for our mathematical model are described. We find that there are seven important non-dimensional parameters which characterize the ash flow and which are the Jeffreys number J_e, the density ratio G, the d namic pressure parameter H, the initial velocity ratio $\bar{u}_o$, the ratio of specific heats of the gas γ, the ratio of specific heat of solid particles to that of the gas at constant pressure δ and the Prandtl number. Among the seven parameters, the Jeffreys number is the most important one which is the ratio of gravitational force to viscous force. Hence Jeffreys number for terrestrial ash flow is larger than that for lunar ash flow.

Numerical solutions for special ash flow with and without heat transfer are presented in which the dynamic pressure parameter and the Prandtl number may drop out. The variations of pressure p, temperature T, velocities of gas and solid particles u_g and u_p, and the volume fraction of the solid particles Z with altitude are plotted for various values of the non-dimensional parameters J_e, $\bar{u}_o$, G and δ.

For isothermal ash flow, the large pressure drop occurs in the dense phase region of low altitude and large volume fraction for large values

of Jeffreys number while the large pressure drop occurs in the dilute phase region of high altitude and small volume fraction for small values of Jeffreys number. Hence the dilute phase is important in the lunar ash flow.

For ash flow with heat transfer, the influence of heat transfer becomes important for the case of small initial velocity $\bar{u}_o$ and for the case of gas of large heat capacity, i.e., small value of δ. For instance, for lunar ash flow with small initial velocity, the effect of the heat transfer would make the whole layer of ash flow more compact together than the corresponding isothermal case. The influence of the heat transfer for the case with hydrogen as the gas species is much larger than that with steam as gas species.

Symbols

b	rate factor of emission of gas from the solid material
$c_{p,v}$	specific heat of gas at constant pressure and constant volume respectively
c_s	specific heat of the solid particles
f	defined by Eq. (54)
F_r	Froude number
g	gravitational constant
G	density ratio of gas and solid particle
h	surface distance between nearby particles
H	dynamic pressure parameter
H_s	local scale height
H_{S_M}	local scale height of mixture of gas and solid particles
J_e	Jeffreys number
K_T	thermal frictional coefficient
L	characteristic length of ash flow
m	molecular weight of the gas
N	an integer
p	pressure
P_r	Prandtl number
r_p	radius of solid particles
R	universal gas constant
R_e	Reynolds number
T	temperature
u	velocity
V_c	characteristic velocity of ash flow
y	altitude

y_m minimum level where fluidization begins

y_c critical level of fluidization beyond which $\bar{u}_p \equiv 0$

Z volume fraction of the solid particles

γ ratio of c_p and c_v

ρ_g , ρ_{sp} density of the gas and the solid particles respectively

δ ratio of c_s and c_p

μ dynamic viscosity of the gas

κ_g coefficient of heat conductivity of the gas

σ_p source function of the gas

Subscripts

g for gas

p for solid particles

0 condition at $y = 0$

1 condition at $y = y_m$

Superscript

- for non-dimensional quantities

I INTRODUCTION

Many geological phenomena can be explained by ash flows. For instance, one of the major processes to account some features of lunar soils is the ash flow[1]. The formation of lunar surface features my be due to the results of lunar ash flows[2]. Hence the analytical treatment of ash flow should improve our understanding of many geological and astro-geological phenomena.

By ash flow, we mean the flow of a mixture of a gas and small solid particles (ash) such that the solid particles have been fluidized and behave like a pseudo-fluid. Thus from the point of view of fluid dynamics, the ash flow is a two phase flow of a mixture of a gas and a pseudo-fluid of small solid particles. The mathematical theory of such a two phase flow is still in a developing stage. In reference 3, the senior author (Pai) gave a review of the fundamental equations of the mixture of a gas and small solid particles. In general, the behavior of the flow of ash depends on the flow rate of the gas. In lunar ash flow, the gas may be produced from a great explosion or a great meteorite impact. Roughly, we may divide the ash flow into two stages: when the flow rate of the gas is above a first critical value, some of the small solid particles on a fixed bed may first move with the gas flow. As the flow rate increases, the amount of the solid particles moved with the gas flow increases. We may call this initial stage, the sedimentation stage[4], in which the solid particles are transported by the gas flow. In the sedimentation stage, the behavior of the solid particles acts as individual particles and their motion depends mainly on their individual physical

properties such as its size, shape, density as well as relative position between particles.

When the rate of the fluid flow reaches a second critical value, called the flow of fluidization, the character of the solid particles changes abruptly to a pseudo-fluid. The flow of the solid particles (ash) has a similar behavior of the flow of an ordinary fluid and the physical properties of individual solid particles are not very important but they contribute only to the average properties of the ash as a whole. In this paper, we consider only the case that the flow of ash may be considered as the flow of a pseudo-fluid.

In genereal, the ash flow problem is very complicated. In order to obtain some essential features of lunar ash flow, it is advisable to study first some simple configurations. Hence we shall follow O'Keefe-Adams[5] to study one dimensional steady flow of a mixture of a gas and small solid particles for both the case on the moon and on the earth. Our analysis is an improvement of O'Keefe-Adams' analysis by including the velocity of the solid particles and the heat transfer in the mixture. Hence O'Keefe Adams' result is a special case of our general treatment.

Our mathematical model is shown in Fig. 1 in which we assume that the gas is coming out from ground upward into free space. We take $y = 0$ at the top of the fixed bed. The gas velocity will increase with altitude y. Between $y = 0$ and $y = y_m$, the mixture of the gas and solid particles is in the sedimentation stage, in which the ash moves but it can not be considered as a pseudo-fluid. When the altitude is higher than $y = y_m$, the ash is fluidized. We are going to find the distribution of pressure, temperature and velocities of the gas and the ash as well as the volume fraction of the ash, under various conditions.

Because the temperature of the gas T_g and that of the solid particles T_p may be different and the velocity of the gas u_g and that of the solid particles u_p may also be different, we have to consider seven variables in a general one-dimensional ash flow. These seven variables are (1) the temperature of the gas T_g (2) the temperature of the pseudo-fluid of solid particles T_p, (3) the velocity of the gas u_g, (4) the velocity of the pseudo-fluid of solid particles u_p, (5) the species density of the gas ρ_g, (6) the pressure of the mixture p and (7) the volume fraction of solid particles in the mixture Z. In section II, the seven fundamental equations which govern these seven variables are given. These fundamental equations should be solved with proper boundary conditions which are discussed in section II too.

Before we solve the fundamental eqautions for the boundary conditions, we first find the important non-dimensional parameters which characterize the ash flow in section III. These non-dimensional parameters are very useful in correlation of our numerical results.

We solve the fundamental equations under various conditions in section IV and the numerical results are discussed in section V.

II. FUNDAMENTAL EQUATION OF ONE-DIMENSIONAL STEADY ASH FLOW AND THEIR BOUNDARY CONDITIONS.

Since we do not consider the transition region near a solid boundary, we may assume that the viscous stress and heat conduction of the gas and those of the pseudo-fluid of solid particles are negligible. From reference 3, we find that the fundamental equations of one dimensional steady ash flow as follows:

(1) Equation of state of the gas:

$$p = \frac{R}{m} \rho_g T_g \tag{1}$$

where R is the universal gas constant, m is the molecular weight of the gas. Eq. (1) is simply the perfect gas law. We write Eq (1) in such a form that we may study the effect of different gaseous species by varying the value m.

(2) Equations of continuity. The conservation of mass of the pseudo-fluid of solid particles and that of the gas in the mixture give respectively the equation of continuity of these species as follows:

$$\frac{d}{dy} [Z \rho_{sp} u_p] = - \sigma_p \tag{2}$$

$$\frac{d}{dy} [(1 - Z)\rho_g u_g] = \sigma_p \tag{3}$$

where ρ_{sp} is the species density of the solid particles and is considered to be a constant, σ_p is the source term of the gas, i.e., some of the gas may be emitted from the solid particles and y is the vertical distance from the surface of earth, moon or other planet in our problem as shown in Fig. 1. The y-direction is coincided with the flow direction and is opposite to the direction of gravitational acceleration. We assume that the source term may be expressed as

$$\sigma_p = bZ \rho_{sp} \tag{4}$$

where b is the rate factor of emission of the gas from the solid particles and is assumed to be a constant in our analysis.

(3) Equations of motion. The equation of motion for the mixture as a whole is

$$(1 - Z)\rho_g u_g \frac{du_g}{dy} + Z\rho_{sp} u_p \frac{du_p}{dy} = - \frac{dp}{dy} - [(1 - Z)\rho_g + Z\rho_{sp}]g \qquad (5)$$

where g is the gravitational acceleration. We need another equation of motion of either the gas or the pseudo-fluid of solid particles. As discussed in Reference 3 and Appendix I, the difficulty in writing down such an equation of motion lies in the proper expression for the term of interaction force between the gas and the solid particles. At low Reynolds number flow where the inertial terms may be neglected and for negligible volume fraction Z of the solid particles, Stokes law may be used for the interaction force. But for the ash flow under consideration, the values of Z may vary from 0.5 to 0. At finite values of Z, the validity of all know theoretical results[6,7] for the interacion force are not very satisfactory. Thus some empirical relation is desired. From the experimental results of Ergun[8], Leva[9], Rowe[10] and others given in Reference 7, a new empirical equation for the pressure gradient in a mixture of fluid-solid two-phase flow were obtained as follows (see Appendix I for detailed discussion):

$$\frac{dp}{dy} = - \frac{Z}{(1-Z)^2} \frac{9\mu}{2r_p^2} (u_g - u_p) \left(1 + \frac{0.68}{h/r_p}\right) = - ZK(u_g - u_p) \qquad (6)$$

where

$$K(Z, r_p, \mu) = \frac{1}{(1 - Z)^2} \frac{9\mu}{2r_p^2} \left(1 + \frac{0.68}{h/r_p}\right) \quad , \qquad (6a)$$

r_p is the average radius of the solid particles and h is the average

distance between the surface of nearby solid particles. As shown in Appendix II, h/r_p in Eq. (6) is a function of Z only if we assume that the solid particles are spheres of radius r_p, i.e.,

$$\frac{h}{r_p} = (1.35\ Z)^{-1/3} - 1 \quad . \tag{7}$$

Eq. (6) is convenient to use because it is a single formula which reduces to Stokes law when Z approaches to zero and, on the other hand, it agrees well with the experimental data of Ergun[8] and Leva[9] and others at finite Z. Thus Eq. (6) covers the whole range of Z which we need. In Eq. (6) the source term of momentum has been neglected. It is a very small term in our analysis.

(4) Equations of Energy. The conservation of energy for the mixture as a whole is:

$$(1-Z)\rho_g u_g (c_p T_g + \frac{1}{2} u_g^2 + gy) + Z\rho_{sp} u_p (c_s T_p + \frac{1}{2} u_p^2 + yg + \frac{p}{\rho_{sp}}) = c_1 \tag{8}$$

where c_p is the specific heat of the gas at constant pressure; c_s is the specific heat of the solid particles and c_1 is a constant which represents the total energy of the mixture and which may be determined by the boundary conditions as will be discussed later. In considering the conservation of energy for the gas, we again have the difficulty in writing down the heat transfer term between the gas and the solid particles for finite values of Z. One way to overcome this difficulty is to assume that Reynolds analogy between heat transfer and drag force may be applied. Thus the thermal friction coefficient may be approximated by the formula:

$$K_T = \frac{3}{2} \frac{\kappa_g}{\mu} K(Z, r_p, \mu) \tag{9}$$

where κ_g is the coefficient of thermal conductivity of the gas, therefore, the energy equation for the gas is

$$\frac{d}{dy}\left[(1-Z)\rho_g u_g (c_p T_g + \frac{1}{2} u_g^2 + gy)\right] = -K_T(T_g - T_p) + bZ\rho_{sp}(c_p T_g + \frac{1}{2} u_g^2 + yg) \ . \tag{10}$$

The last term in Eq. (10) is the energy source of the gas emitted from the solid particles.

Our fundamental equations for one dimensional steady ash flow are Eqs. (1), (2), (3), (5), (6), (8) and (10) for the seven unknowns u_g, u_p, p, ρ_g, Z, T_g and T_p. These fundamental equations are to be solved for appropriate boundary conditions. The problem which we are going to solve is shown in Fig. 1. The source of solid particles is underneath the ground. From the general description of two phase flow or fluidization of solid particles[3], we know that when $Z \geq 0.5$, the solid particles may be considered as a fixed bed. For convenience, we take $y = 0$ at the particular level in the fixed bed where $Z = Z_o = 0.5$, We assume that at $y = 0$, the velocity of the gas u_{go} and that of the pseudo-fluid of solid particles u_{po} are known and we set them equal to u_1 and u_o respectively. Furthermore, the pressure p_o and the volume fraction of the solid particles Z_o are also known. We assume that at $y = 0$, the temperatures of the gas and the solid particles are in equilibrium at T_o. Therefore, our boundary conditions are:

at $y = 0$:

$$u_{go} = u_1 \ , \qquad u_{po} = u_o$$
$$p = p_o \ , \qquad Z = Z_o = 0.5 \text{ (average)}$$
$$T_{po} = T_{go} = T_o \ . \tag{11}$$

A few words should be said about the boundary value u_o. Since we assume that all the solid particles come from the ground and none comes from outer space, the velocity of the pseudo-fluid of solid particles should not be negative. If $u_o = 0$, the integration of equation of continutity, Eq. (2), would give negative value of u_p for $y > 0$, which is contradictory to our physical picture. Hence we should assume that $y \geq 0$, $u_p \equiv 0$ when $u_o = 0$. Similarly, u_p may decrease with increasing altitude, for certain small values of u_o (see numerical example later). For such case, even though $u_o > 0$ at $y = 0$, u_p may reduce to zero at $y = y_c > 0$. By the same argument as in the case of $u_o = 0$, we should assume that $u_p \equiv 0$ for $y > y_c$. On the other hand, the assumption of $u_p \equiv 0$ for $y > 0$ or $y > y_c$ suffers a defect from the physical picture too. Since the gas is emitting at all time from the solid particles at the expense of the mass of solid particles when $u_p \equiv 0$, a local volume fraction of the solid particles can not be steadily maintained. (Note that we have dropped the continuity equation of the solid particles when we assume $u_p \equiv 0$). Strictly speaking, in such a case, we do not have steady flow. However, in view of the small value of the rate factor b, we may accept our quasi-steady analysis as a good first approximation to the unsteady flow problem.

There is no restriction on the initial value of the velocity of the gas u_1. For simplicity, in the numerical examples calculated in this paper, we assume $u_1 = u_o$ which means that we have equilibrium condition at $y = 0$. The assumption of initially equilibrium in temperatures of the gas and solid particles will later be shown to prevail throughout the entire flow field.

In general, the volume fraction of solid particles Z decreases with increase of altitude y. We set the minimum fluidization level[9] $y = y_m$ arbitrarily at $Z = 0.4$. When $y > y_m$, the solid particles may be considered as a pseudo-fluid and our fundamental equations (1) to (10) hold true.

III. IMPORTANT NON-DIMENSIONAL PARAMETERS.

Before we solve our fundamental equations (1) to (10) under the boundary conditions (11), we first find the important non-dimensional parameters which characterize the ash flows from our fundamental equations and boundary conditions. We introduce the following non-dimensional quantities:

$$\bar{p} = \frac{p}{p_o}, \quad \bar{\rho}_g = \frac{\rho_g}{\rho_{go}} = \frac{R\,T_o}{m\,p_o}\rho_g, \quad \bar{y} = \frac{y}{L}$$

$$\bar{u}_g = \frac{u_g}{V_c}, \quad \bar{u}_p = \frac{u_p}{V_c}, \quad \bar{T}_g = \frac{T_g}{T_o}, \quad \bar{T}_p = \frac{T_p}{T_o} \tag{12}$$

where the bar refers to the non-dimensional quantities, the characteristic length L is taken as follows:

$$L = \frac{p_o}{\rho_{sp}\, g} \quad . \tag{13}$$

Hence L is a modified scale height which is taken as a unit length in our analysis. The characteristic velocity V_c is defined by the following relation

$$V_c = \frac{bRT_o}{mg} \quad . \tag{14}$$

The characteristic velocity V_c measures the significance of the emission of gas from the solid particles. This is one of the basic physical phenomena in our prbolem.

Substituting the expressions (12) into Eqs. (1), (2), (3), (5), (6), (8) and (10), we have the following corresponding non-dimensional fundamental eqautions in which the non-dimensional parameters J_e , G , H, γ , δ and P_r are defined in Eqs. (24) to (31) as follows:

$$\bar{p} = \bar{\rho}_g \bar{T}_g \tag{15}$$

$$\frac{d}{d\bar{y}} (Z \bar{u}_p) = - \frac{Z}{G} \tag{16}$$

$$\frac{d}{d\bar{y}} [(1 - Z)\bar{\rho}_g \bar{u}_g)] = Z \tag{17}$$

$$H\left[\frac{1-Z}{G} \bar{\rho}_g \bar{u}_g \frac{d\bar{u}_g}{d\bar{y}} + Z \bar{u}_p \frac{d\bar{u}_p}{d\bar{y}}\right] = - \frac{d\bar{p}}{d\bar{y}} - \frac{(1-Z)\bar{\rho}_g}{G} - Z \tag{18}$$

$$\frac{d\bar{p}}{d\bar{y}} = - \frac{Z}{(1-Z)^2} \frac{9}{2J_e} \left(1 + \frac{0.68}{h/r_p}\right) (\bar{u}_g - \bar{u}_p) \tag{19}$$

$$(1-Z)\bar{\rho}_g \bar{u}_g \left[\bar{T}_g + \frac{\gamma-1}{\gamma G} (\frac{H}{2} \bar{u}_g^2 + \bar{y})\right] + ZG \bar{u}_p \left[\delta \bar{T}_p + \frac{\gamma-1}{\gamma G} (\frac{H}{2} \bar{u}_p^2 + \bar{y} + \bar{p})\right] = \bar{c}_1 \tag{20}$$

$$(1-Z)\bar{\rho}_g \bar{u}_g \frac{d\bar{T}_g}{d\bar{y}} = \frac{27}{4} \frac{G}{P_r J_e H} \frac{1}{(1-Z)^2} \left(1 + \frac{0.68}{h/r_p}\right) (\bar{T}_g - \bar{T}_p) \tag{21}$$

and the boundary conditions are

at $\bar{y} = 0$:

$$\bar{u}_{go} = \bar{u}_{po} = \bar{u}_o$$
$$\bar{p} = 1 \ , \quad Z_o = 0.5 \tag{22}$$
$$\bar{T}_{po} = \bar{T}_{go} = 1$$

From Eqs. (15) to (22), we have obtained seven independent non-dimensional parameters: $\bar{u}_o$, J_e , G , H , γ , P_r and δ . The relative importance of these parameters and their meanings are discussed as follows:

(1) Initial velocity ratio $\bar{u}_o$ which is defined as

$$\bar{u}_o = \frac{u_o}{V_c} \quad . \tag{23}$$

In the ash flow under consideration, there are two possible reference velocities which represent the sources of the gas in the flow field. One is due to the emission of the gas from the solid particles in the flow field considered which is represented by the characteristic velocity V_c of Eq. (14). In this report, we consider this case in which the main source of the gas comes from the solid particles in the flow field. Hence we use the characteristic velicity V_c as our reference velocity. However, in the actual physical situation the release of gases from the solid particles may take place before they enter the flow field, or in other words, before they leave the fixed bed of Fig. 1 and then we have some gases coming from outside of the flow field considered. The amount of these gases may be represented by the initial gas velocity u_o , which is independent of the rate factor b . For problems in which V_c is larger than u_o , we should use V_c as a reference velocity as in Eq. (12). On the other hand, if the gas comes mainly from the ground, we have $u_o > V_c$ and then we should use u_o as our reference velocity. In this case, the non-dimensional velocity should be

$$u_g^* = \frac{u_g}{u_o} = \frac{\bar{u}_g}{\bar{u}_o} \quad . \tag{23a}$$

Hence the non-dimensional velocity in terms of V_c is equal to that in terms of u_o times the initial velocity ratio $\bar{u}_o$.

(2) Jeffreys number J_e which is defined as

$$J_e = \frac{\rho_{sp}\, r_p\, g^2}{\mu(b\, \frac{R}{m}\, T_o)} = \frac{R_e}{F_r} = \frac{\text{gravitational force}}{\text{viscous force}} \tag{24}$$

where

$$R_e = \frac{\rho_{sp}\, r_p\, V_c}{\mu} = \text{Reynolds number} \tag{25}$$

$$F_r = \frac{V_c^2}{r_p g} = \text{Froude number} \tag{26}$$

Since Reynolds number R_e represents the ratio of inertial force to viscous force and Froude number represents the ratio of the inertial force to gravitational force, the Jeffreys number represents the ratio of gravitational force to the viscous force. The importance of Jeffreys number in astrogeological problem was first pointed out by O'Keefe[11], who suggested the name of Jeffreys number. In our problem, the main forces are the gravitational force and viscous force. Hence Jeffreys number is the most important parameter in our problem. A parameter F was first introduced by O'Keefe and Adams in Lunar ash flow[5] such that $78.1\ F = J_e$ of our paper. The only difference between their F and our J_e of Eq. (24) is a numerical constant.

It is interesting to notice that if we use u_o as our reference velocity, we should replace V_c in Eq. (24) by u_o, and then the corresponding Jeffreys number becomes

$$J_e^* = \frac{\rho_{sp}\, r_p^2\, g}{u_o} = \frac{J_e}{\bar{u}_o} \tag{24a}$$

J_e^* is simply the ratio of J_e and $\bar{u}_o$. We do not introduce any new parameters but use a different combination of old parameters.

(3) Density ratio G which is defined as

$$G = \frac{\rho_{sp}}{\rho_{go}} \quad . \tag{27}$$

The parameter G is the ratio of the density of the ash to the initial density of the gas. This parameter G represents the effect of the weight of the gas in the ash flow.

(4) Dynamic pressure parameter H which is defined as

$$H = \frac{\rho_{sp} V_c^2}{p_o} \quad . \tag{28}$$

The parameter H is essentially the ratio of the dynamic pressure based on the reference velocity V_c to the initial static pressure p_o. Hence the parameter H shows the effect of inertial terms. If H is very small, we may neglect all the inertial terms in Eqs (18) and (20). If we use u_o as a reference velocity, the dynamic pressure parameter should be

$$H^* = \frac{\rho_{sp} u_o^2}{p_o} = H \bar{u}_o^2 \quad . \tag{28a}$$

Again H^* is simply a combination of H and $\bar{u}_o^2$.

(5) Gas property parameter γ which is defined as

$$\gamma = \frac{c_p}{c_v} \tag{29}$$

where γ represents the ratio of the specific heat of the gas at constant pressure c_p to the specific heat of the gas at constant volume c_v. Hence it is a parameter solely for the gas in the ash flow. For most ash flow, we may assume that γ is a constant in the problem considered.

(6) Specific heat ratio δ which is defined as

$$\delta = \frac{c_s}{c_p} \quad . \tag{30}$$

This parameter indicates the relative importance of heat capacity between the solid particles and the gas and it is important in the determination of temperature distribution of the mixture.

(7) Prandtl number of the gas P_r which is defined as

$$P_r = \frac{\mu c_p}{\kappa_g} \quad . \tag{31}$$

The Prandtl number P_r is important in the study of heat transfer between species. In most cases, we may assume that $P_r = 1$.

We note that the first four parameters $\bar{u}_o$, J_e , G and H are due to the dynamics of the ash flow. Hence they always exist whether the ash flow is with or without heat transfer. The last three parameters γ, δ and P_r are due to the thermodynamics of the ash flow. Hence in the isothermal ash flow, we need to consider the four parameters $\bar{u}_o$, J_e , G and H while in non-isothermal case, all the seven parameters should be considered.

Among these seven parameters in our problem, some of the parameters are not important and may be neglected. For instance, in most ash flows, the factor b of rate of emission of gas is a very small quantity. Thus the characteristic velocity V_c would be a small quantity too (see Fig. 2). As a result, the dynamic pressure parameter H is also a small quantity (see Fig. 3). In other words, the inertial terms in the fundamental equations may be neglected which means $H \cong 0$. For very small H , Eq. (21) gives that $T_g \cong T_p$. For the case of $T_g = T_p$, the Prandtl number P_r will disappear in the resultant fundamental equations. Hence for the general case of non-isothermal ash flow, we need to consider five parameters $\bar{u}_o$, J_e , G , γ and δ .

It is interesting to notice that in O'Keefe and Adams paper[5], they consider the limiting case of isothermal ash flow where $H = 0$, $\bar{u}_o = 0$ and $G \to \infty$. Hence they have only one important parameter J_e (or their F). As discussed before, $\bar{u}_o = 0$ requires $\vec{u}_p \equiv 0$ while $G \to \infty$ requires that the weight of the gas is totally neglected. These two conditions are generally true in the dense phase region of the ash flow (see section III and IV). Thus O'Keefe and Adams[5] results represent one of the limiting cases of our more general treatment of lunar ash flow.

IV. METHOD OF SOLUTION

As pointed out by O'Keefe and Adams[5], the cooling of an ash flow is a conspicuously slow process. From our experience in the study of general fluid dynamic problems, the isothermal flow would give many important features of the flow field. In most cases, the effects of heat transfer would affect only quantitatively the results of the flow field but give essentially the same features of the flow field qualitatively. Hence we shall first study the isothermal case in part (a) of this section. The effect of heat transfer will affect the flow field quantitatively in certain cases. Hence we shall study the effect of heat transfer on ash flow in part (b) of this section.

(a) Isothermal ash flow. In isothermal ash flow, we let $T_g = T_p = T_o$ or $\bar{T}_g = \bar{T}_p = 1$ in the whole flow field. Hence we do not need to study the temperature distribution. We investigate only the five unknowns: ρ_g, p, Z, u_g and u_p which are governed by equations (15) to (19). Furthermore, we shall consider the case $H \cong 0$ so that our fundamental equations (15) to (19) become:

$$\bar{p} = \bar{\rho}_g \tag{32a}$$

$$\frac{d}{d\bar{y}} (Z\, \bar{u}_p) = - \frac{Z}{G} \tag{32b}$$

$$\frac{d}{d\bar{y}} [(1 - Z)\, \bar{p}\, \bar{u}_g] = Z \tag{32c}$$

$$\frac{d\bar{p}}{d\bar{y}} = - Z \left[1 + \frac{(1 - Z)\bar{p}}{Z\, G} \right] \tag{32d}$$

$$\frac{d\bar{p}}{d\bar{y}} = - \frac{Z}{(1-Z)^2} \frac{9}{2J_e} \left(1 + \frac{0.68}{h/r_p} \right) (\bar{u}_g - \bar{u}_p) \quad . \tag{32e}$$

The boundary conditions are

$$\text{at } \bar{y} = 0 : \quad \bar{u}_{go} = \bar{u}_{po} = \bar{u}_o , \quad \bar{p} = 1 , \quad Z_o = 0.5 \quad . \tag{32f}$$

In Fig. 1, we divide the flow field into three regions: dense phase, transition phase and dilute phase for convenience. By dense phase, we mean that the volume fraction Z of the solid particle is not negligible in comparison to unity. Furthermore, if the density ratio G is large, we may obtain simple analytic solution for the dense phase region from our fundamental equations (32), because the effect of the weight of the gas is negligibly small. By dilute phase, we mean that the volume fraction Z becomes so small that we can not neglect the weight of the gas any more nor the velocity of the solid particles. The region between the dense and dilut phase is known as the transition phase. It should be noticed that there are no definite boundaries between these phases. Furthermore, our fundamental equations (32) hold true for all these three phases.

We obtain the general solutions of Eqs. (32) by numerical solutions which are valid for all these three phases.

(i) Dense phase region:

In the dense phase region, Z is not negligible in comparison to unity. The density ratio G is in general a large quantity of 10^4 (see numerical example). As a result, $(1 - Z)p/ZG << 1$ and Eq. (32) becomes

$$\frac{d\bar{p}}{d\bar{y}} = Z \quad . \tag{33}$$

Now, substituting Eq. (33) into Eqs. (32b) and (32c) and integrating the resultant equations (32f), we have

$$\bar{u}_g = \frac{1 - \bar{p}}{\bar{p}(1 - Z)} = \frac{\bar{u}_o(1 - Z_o)}{\bar{p}(1 - Z)} \tag{34}$$

and

$$\bar{u}_p = \frac{1}{GZ}(\bar{p} - 1) + \frac{Z_o \bar{u}_o}{Z} \quad . \tag{35}$$

It is interesting to notice that when $\bar{u}_o = 0$ or small (of the order of $1/G$, say), the ratio of u_g/u_p is of the order of G. Since $G >> 1$, $u_p << u_g$ in the dense phase. This justifies the validity of O'Keefe and Adams' assumption that the solid particles do not move in their solution[5] for the dense phase of the ash flow.

Substituting Eqs. (33) to (35) into Eqs. (32e), we obtain an algebraic equation for $\bar{p}$ and Z as follows:

$$\bar{p}^2 + Q(Z)\,\bar{p} - W(Z) = 0 \tag{36}$$

where

$$Q(Z,J_e,G) = GZ\left[\frac{1}{1-Z} + \frac{1}{\bar{K}(Z,J_e)}\right] - 1 - Z_o\,\bar{u}_o\,G \tag{36a}$$

$$W(Z,G) = \frac{GZ}{1-Z}[1-\bar{u}_o(1-Z_o)] \tag{36b}$$

$$\bar{K}(Z,J_e) = \frac{9}{2J_e}\frac{1}{(1-Z)^2}\left(1 + \frac{0.68}{h/r_p}\right) \tag{36c}$$

and h/r_p in Eq. (36c) is given by Eq. (7). The physical possible solution of $\bar{p}$, i.e., $\bar{p} > 0$, given by Eq. (36) is

$$\bar{p} = \frac{1}{2}\left[-Q + (Q^2 + 4W)^{\frac{1}{2}}\right] \quad . \tag{37}$$

Eqs. (33) to (37) describe the complete flow field of the dense phase region in which the weight of the gas is negligible in comparison with that of solid particles in any element of volume of the mixture. Since $\bar{\rho}_g = \bar{p}$ as given by Eq. (32a). We have the solutions for all the five variables $\bar{\rho}_g$, $\bar{p}$, $\bar{u}_g$, $\bar{u}_p$ and Z in the dense phase region.

To obtain numerical results of the solution of Eqs. (33) to (37), it is convenient to use Z as an independent variable. For a given value of Z, we can easily obtain $\bar{p}(z)$ from Eq. (37), then $\bar{u}_g(Z)$ from Eq. (34) and $\bar{u}_p(Z)$ from Eq. (35). Finally the vertical distance $\bar{y}$ may be obtained by integrating Eq. (33) as follows:

$$\bar{y} = -\int_{Z_1}^{Z} \frac{1}{Z}\left(\frac{d\bar{p}}{dZ}\right)dz + \bar{y}_1 \tag{38}$$

where subscript 1 refers to the values at a reference altitude, i.e., at $Z = Z_1$, $\bar{y} = \bar{y}_1$. In general the solutions $\bar{p}(Z)$, $\bar{u}_g(Z)$, $\bar{u}_p(Z)$ and $\bar{y}(Z)$ depend on the parameters $\bar{u}_o$, J_e and G. We shall discuss the numerical results in section V.

Let us compare our solution in the dense phase region with those of O'Keefe-Adams in reference 5. They considered the case $\bar{u}_o = 0$ only. For the case $\bar{u}_o = 0$, Eqs. (34) and (35) show that

$$\frac{\bar{u}_g}{\bar{u}_p} = 0(G) \quad . \tag{39}$$

Since G is a large quantity, it is proper to assume that $\bar{u}_p = 0$ in the whole region of dense phase. At the same time, Eqs. (34) and (36) become respectively

$$\bar{u}_g = \frac{1 - \bar{p}}{\bar{p}(1 - Z)} \tag{40a}$$

and

$$\bar{p} = \frac{1}{1 + \frac{(1 - Z)}{K}} \quad . \tag{40b}$$

Eqs. (40) are essentially the same results as given in reference 5. In Eqs. (40), we have only one non-dimensional parameter J_e which is in the expression of $\bar{K}$.

It is interesting to notice that if $\bar{u}_o$ is not zero but of the order of $1/G$ which is a small quatity, we may still neglect $\bar{u}_p$ in the study of the flow field of the dense phase region. However if $\bar{u}_o$ is of the order of unity or larger, we can not neglect $\bar{u}_p$ even in the dense phase region. In our numerical results, we consider only the cases that $\bar{u}_o$ is of the order of $1/G$ in order to show some essential differences between the dense phase and the dilute phase of the flow field.

It is generally assumed[5,9] that the fluidization begins at $Z = 0.4$. When $\bar{u}_o$ is of the order of $1/G$, we may use Eq. (40b) to determine the pressure p_1 at the position of the beginning of fluidization, i.e.,

$$\bar{p}_1 = \frac{1}{1 + 0.59\ \frac{J_e}{37.5}} \quad . \tag{41}$$

It is further assumed that between the top of the fixed bed $\bar{y} = 0$ and the level of minimum fluidization an average value of $Z = 0.5$ may be used. Hence Eq. (33) gives

$$\bar{y}_1 = 2\ (1 - \bar{p}_1) \tag{42}$$

i.e., the altitude at which $Z = Z_1 = 0.4$, $\bar{y} = \bar{y}_1$.

(ii) Dilute phase region

As the flow and solid particles move upward, both the pressure $\bar{p}$ and the volume fraction of solid particles Z decrease with altitude $\bar{y}$ while the gas velocity $\bar{u}_g$ increases with $\bar{y}$. Eventually, when Z becomes so small that we can not neglect the weight of the gas any more nor the velocity of the solid particles $\bar{u}_p$ (if $\bar{u}_p$ does not go to zero). This is the dilute phase of the ash flow. We have to integrate Eqs. (32a) to (32e) numerically with the boundary condition Eq. (32f). However, if we limit ourselves to the case that $\bar{u}_o$ is of the order of $1/G$, some simplifications may be made. For instance, the total equation of continuity of the mixture may be obtained by adding Eqs. (16) and (17) and integrating the resultant equation with respect to $\bar{y}$ as follows:

$$(1 - Z)\bar{u}_g\ \bar{p} + \bar{u}_p\ ZG = (1 - Z_o)\bar{u}_o + \bar{u}_o Z_o G \cong \bar{u}_o Z_o G \tag{43}$$

because $(1 - Z_o)\bar{u}_o << \bar{u}_o Z_o G$. Hence Eq. (43) gives

$$\bar{u}_p = \frac{1}{ZG}\left[\frac{1}{2}\ \bar{u}_o G - (1 - Z)\bar{u}_g \bar{p}\right] \tag{44}$$

where we take $Z_o = \frac{1}{2}$. From Eqs. (32d), (32e) and (44), we have

$$\bar{u}_g = \frac{1}{\bar{K}} + \frac{\bar{u}_o}{2Z}\left[1 + (1 - Z)\frac{\bar{p}}{ZG}\right]^{-1} \quad . \tag{45}$$

It should be noticed when $\bar{u}_o = 0$, because of our assumption of $\bar{u}_p \equiv 0$ in the whole flow field, Eq. (45) reduces to

$$\bar{u}_g = \frac{1}{\bar{K}}\left[1 + (1 - Z)\frac{\bar{p}}{ZG}\right] \quad , \quad \bar{u}_o = 0 \quad . \tag{45a}$$

It is again convenient to use Z as the independent variable in the numerical integration for the dilute phase. From Eqs. (32c) and (32d), we have

$$\frac{d\bar{p}}{dz} = \frac{\bar{K}\left[\frac{\bar{u}_g}{(1 - Z)} + \frac{\bar{u}_p}{Z}\right] + (\bar{u}_g - \bar{u}_p)\frac{d\bar{K}}{dZ} + \frac{\bar{p}}{GZ^2}}{\frac{1-Z}{G} + \bar{K}\left\{\frac{1}{\bar{p}(1-Z)}\left[\frac{1}{1 + \frac{(1-Z)\bar{p}}{GZ}} + (1-Z)\bar{u}_g\right] + \frac{1}{GZ + (1-Z)\bar{p}}\right\}} \tag{46}$$

and

$$\bar{y} = -\int_{Z_1}^{Z} \frac{\frac{d\bar{p}}{dZ}}{Z + \frac{(1-Z)\bar{p}}{G}}\, dZ + \bar{y}_1 \tag{47}$$

where $\bar{K}$ is a function of Z given by Eq. (36c) for a constant J_e . $\bar{u}_p(Z,\bar{p})$ and $\bar{u}_g(Z,\bar{p})$ are given by Eqs. (44) and (45) respectively. Eqs. (46) and (47) must be integrated numerically. Numerical solutions have been obtained by the help of high speed computer UNIVAC 1108 of the Computer Science Center of University of Maryland.

(b) Ash Flow with Heat Transfer

Even though the isothermal ash flow gives qualitatively the general behavior of flow field of ash flow, the effect of heat transfer would affect quantitatively the flow field of a lunar ash flow which may be very

important in the final interpretation of the features of lunar soil. Hence in this section we consider the ash flow with heat transfer.

With heat transfer, we have to solve Eqs. (15) to (21) with the boundary conditions (22). Again, we neglect all the inertial terms by putting $H = 0$ in Eqs. (18) and (20). If we put $H = 0$ in Eq. (21), we see that we must have $\bar{T}_g \equiv \bar{T}_p$ since the temperature gradient of the gas in the flow field can not be infinite. Even though H is not actually zero, we found in one numerical calculation that the constant in the right hand side of Eq. (21) is of the order of

$$\frac{27}{4} \cdot \frac{G}{P_r J_e H} \sim 10^6$$

for ash flow under our consideration. Since the rest of the terms in Eq. (21) are of the order of unity, for all practical purpose we may set

$$\bar{T}_g = \bar{T}_p = \bar{T} \quad . \tag{48}$$

In other words, the heat transfer between the gas and the solid particles in our cases is so fast that they are practically in local equilibrium everywhere throughout the flow field and we have only one temperature $\bar{T}$.

The constant c_1 in Eq. (20) may be determined from the condition given in Eq. (22). However, since the solid particles are not yet fluidized in the sedimentation region of $\bar{y} = 0$ to $\bar{y} = \bar{y}_1$, our knowledge of the thermal situation in this sedimentation region is rather meager. In order to get some definite idea of the thermal situation in the flow field $\bar{y} > \bar{y}_1$, we may replace the actual sedimentation by an average temperature in this thin layer. As a result, our boundary condition becomes

$$\bar{y} = \bar{y}_1;\ Z = Z_1 = 0.4;\ \bar{u}_p = \bar{u}_{p1},\ \bar{u}_g = \bar{u}_{g1},\ \bar{p} = \bar{p}_1,\ \bar{T}_g = \bar{T}_p = 1 \quad . \tag{49}$$

With this thermal boundary condition (49), the total energy constant $\bar{c}_1$ is

$$\bar{c}_1 = Z_o G\bar{u}_o + (\delta - 1)0.4\ G\bar{u}_{p1} + \left(Z_o G\bar{u}_o \frac{\bar{y}_1}{G} + 0.4\ \bar{u}_{p1}\ \bar{p}_1\right) \frac{\gamma-1}{\gamma} \quad . \tag{50}$$

With the help of Eqs. (44) and (48), Eq. (20) gives

$$\bar{T}_g = \bar{T} = \frac{\bar{c}_1' - \frac{\gamma - 1}{\gamma G}\left(\bar{y} + \frac{Z\ \bar{u}_p}{Z_o\ \bar{u}_o}\ \bar{p}\right)}{1 + (\delta - 1)\ Z\ \bar{u}_p / Z_o \bar{u}_o} \tag{51}$$

where

$$\bar{c}_1' = \frac{\bar{c}_1}{Z_o G\bar{u}_o} = 1 + (\delta-1)\ \frac{0.4\ \bar{u}_{p1}}{Z_o\ \bar{u}_o} + \frac{\gamma-1}{\gamma G}\left[\bar{y}_1 + \frac{0.4\ \bar{u}_{p1}}{Z_o\ \bar{u}_{p1}}\ \bar{p}_1\right] \quad . \tag{50a}$$

Eqs. (15), (16), (17), (32d), (32e) and (51) are the fundamental equations for one dimensional steady ash flow with heat transfer which governs the six unknowns $\bar{p}$, $\bar{T}$, $\bar{\rho}_g$, $\bar{u}_g$, $\bar{u}_p$ and Z with the boundary conditions (22) or (44). Again in our numerical calculations, we use Z as the independent variable. After some algebraic manipulation, we obtain the following equations for numerical integraton:

$$\frac{d\bar{p}}{dZ} = \frac{A_8\left(1 - \frac{\bar{\rho}_g}{\bar{T}}\ A_2\right) + \frac{A_9\ A_6\ \bar{\rho}_g}{\bar{T}}}{1 - \frac{1}{\bar{T}}\left[A_7\bar{\rho}_g + A_9(1 + \bar{\rho}_g A_5)\right]} \tag{52}$$

$$\frac{d\bar{y}}{dZ} = - \frac{d\bar{p}/dZ}{Zf} \tag{53}$$

where

$$f = \frac{(1 - Z)\bar{\rho}_g}{GZ} + 1 \tag{54}$$

$$A_1 = 1 + (\delta - 1) \frac{Z\, \bar{u}_p}{\bar{Z}_o\, \bar{u}_o} \tag{55a}$$

$$A_2 = \bar{c}_1 - \frac{\gamma - 1}{\gamma G} \left(\bar{y} + \frac{Z\, \bar{u}_p}{Z_o\, \bar{u}_o} \bar{p} \right) \tag{55b}$$

$$A_3 = - \frac{Z_o\, \bar{u}_o}{Z^2} + (f-1) \left[\frac{d\bar{K}/dZ}{\bar{K}^2} + \frac{Z_o\, \bar{u}_o}{Z^2 f} - \frac{Z_o\, \bar{u}_o\, \bar{\rho}_g}{GZ^2\, f^2} \right] + \frac{\bar{u}_g\, \bar{\rho}_g}{Z^2 G} \tag{55c}$$

$$A_4 = \frac{Z_o\, \bar{u}_o (1 - Z)\, (f - 1)}{G\, Z^2\, f^2} - \frac{(1 - Z)\, \bar{u}_g}{ZG} \tag{55d}$$

$$A_5 = \frac{\gamma - 1}{G\gamma A_1} \left(\frac{Z\, \bar{u}_p}{Z_o\, \bar{u}_o} - \frac{1}{Zf} \right) \tag{55e}$$

$$A_6 = \frac{1}{A_1\, Z_o\, \bar{u}_o} \left\{ \frac{\gamma-1}{\gamma G} \bar{p}\bar{u}_p + \frac{A_2}{A_1} (\delta-1)\bar{u}_p + A_3 \left[\frac{\gamma-1}{\gamma G} \bar{p}Z + \frac{(\delta-1)ZA_2}{A_1} \right] \right\} \tag{55f}$$

$$A_7 = \frac{A_4}{A_1\, Z_o\, \bar{u}_o} \left[\frac{(\gamma - 1)}{\gamma G} \bar{p}Z + \frac{(\delta - 1)\, Z\, A_2}{A_1} \right] \tag{55g}$$

$$A_8 = f\, \bar{\rho}_g \left\{ \bar{u}_g + (1 - Z) \left[\frac{d\bar{K}/dZ}{\bar{K}^2} + \frac{Z_o\, \bar{u}_o}{Z^2 f} - \frac{Z_o\, \bar{u}_o\, \bar{\rho}_g}{Gf^2\, Z^3} \right] \right\} \tag{55h}$$

$$A_9 = f(1 - Z) \left[\frac{Z_o \bar{u}_o (1 - Z)\, \bar{\rho}_g}{Gf^2\, Z^2} - \bar{u}_g \right] \tag{55i}$$

In addition to Eqs. (52) and (53), Eqs. (15), (44), (45) and (51) must also be used in the numerical integration. It should be noticed

that Eqs. (51) and (52) do not apply for the case $\bar{u}_o \equiv 0$ or $\bar{u}_p \equiv 0$. When $\bar{u}_p \equiv 0$, Eq. (20) becomes

$$(1 - Z)\,\bar{\rho}_g\,\bar{u}_g\left[\bar{T}_g + \frac{\gamma - 1}{\gamma G}\,\bar{y}\right] = \bar{c}_2 \tag{56}$$

and

$$\bar{c}_2 = 0.6\,\bar{p}_1\,\bar{u}_{g1}\left(1 + \frac{\gamma - 1}{\gamma G}\,\bar{y}_1\right) \tag{57}$$

where the boundary condition (49) has been used. Again, we may find analytic solution for the dense phase, where $[1 + (1 - Z)\bar{\rho}_g]/GZ << 1$ and $\bar{y}/G << 1$ and we consider only the case of $\bar{u}_o = 0$ and $\bar{u}_p \equiv 0$. The analytic solutions are

$$\bar{p}(Z) = \frac{\bar{c}_2\,\bar{K}}{(1 - Z)} \tag{58a}$$

$$\bar{u}_g(Z) = \frac{1}{\bar{K}} \tag{58b}$$

$$\bar{\rho}_g(Z) = \frac{(\bar{c}_2 + \bar{p}_1)(1 - Z)\bar{K} - \bar{c}_2\,\bar{K}^2}{(1 - Z)^2} \tag{58c}$$

$$\bar{T}(Z) = \bar{p}/\bar{\rho}_g \tag{58d}$$

where the term $(\gamma - 1)\bar{y}/\gamma G$ was neglected in Eq. (56) and $\bar{K}$ is given by Eq. (36c). We may calculate $\bar{y}$ by Eq. (38). It is interesting to note that in Eq. (58), all the four unknowns $\bar{p}(Z)$, $\bar{u}_g(Z)$, $\bar{\rho}_g(Z)$ and $\bar{T}(Z)$ are functions of Z only. When the weight of the gas can not be entirely neglected and $\bar{y}$ is not necessarily small, we have to solve numerically the following equations for the case $\bar{u}_p \equiv 0$:

$$\frac{d\bar{\rho}_g}{dZ} = \frac{(B_1 f - B_3)}{(fB_2 - B_4)} \tag{59a}$$

$$\frac{d\bar{y}}{dZ} = -\frac{1}{Zf}\frac{d\bar{p}}{dZ} \tag{59b}$$

$$\bar{p} = \frac{\bar{c}_2\,\bar{K}}{(1-Z)f} - \frac{\gamma-1}{\gamma G}\bar{\rho}_g\,\bar{y} \tag{59c}$$

$$\bar{u}_g = \frac{f}{\bar{K}} \tag{59d}$$

where f is given by Eq. (53) and

$$B_1 = \bar{\rho}_g\left[\bar{u}_g + (1-Z)\left(\frac{\bar{\rho}_g}{\bar{K}\,Z^2 G} + \frac{\bar{\rho}_g}{\bar{K}^2}\frac{dK}{dZ}\right)\right] \tag{60a}$$

$$B_2 = (1-Z)\left[\bar{u}_g + \frac{(1-Z)\,\bar{\rho}_g}{\bar{K}\,Z\,G}\right] \tag{60b}$$

$$B_3 = \bar{c}_2\left[\frac{d\bar{K}}{dZ} + \frac{\bar{K}}{(1-Z)} + \frac{\bar{\rho}_g}{fZ^2 G}\right]\Bigg/\left[f(1-Z)\left(1 - \frac{\gamma-1}{\gamma G}\frac{\bar{\rho}_g}{Zf}\right)\right] \tag{60c}$$

$$B_4 = \left(\frac{\bar{c}_2}{Zf^2} + \frac{\gamma-1}{\gamma}\bar{y}\right)\Bigg/\left[G\left(1 - \frac{\gamma-1}{\gamma G}\frac{\bar{\rho}_g}{Zf}\right)\right] \tag{60d}$$

It is easy to show that when $f \to 1$ and $\bar{y}/G \ll 1$, Eqs. (59) reduce to Eqs. (58). Finally, there are cases where $\bar{u}_o \neq 0$ but $\bar{u}_p = 0$ at $y = y_c$ as discussed previously for the isothermal case. When this occurs, we simply put $\bar{u}_p \equiv 0$ for $\bar{y} > \bar{y}_c$ and replace the constant $\bar{c}_2$ by

$$\bar{c}_2^{*} = (1 - Z_c)\,\bar{\rho}_{gc}\,\bar{u}_{gc}\,(\bar{T}_c + \frac{\gamma-1}{\gamma G}\,\bar{y}_c) \tag{61}$$

and continue the computation with Eqs. (59) for $\bar{y} > \bar{y}_c$. In Eq. (61), the subscript c denotes the values at $\bar{y} = \bar{y}_c$.

V. NUMERICAL RESULTS AND DISCUSSIONS

In our numerical calculations, we limit ourselves to the cases $\bar{u}_o = 0(1/G)$ and $H \cong 0$ as discussed in Section III. We shall examine the effects of $\bar{u}_o$, J_e and G with two sets of γ and δ : one for steam and the other for hydrogen gas. The following values have been used in our calculations:

(i) General data

$$g = 980 \ \frac{cm}{sec^2} \text{ for earth}, \quad g = 160 \ \frac{cm}{sec^2} \text{ for moon}$$

$$T_o = 1130 \ ^\circ K \quad . \tag{62a}$$

(ii) For solid particles

$$\rho_{sp} = 2.4 \ gm/cm^3 \ ; \quad r_p = 0.005 \text{ cm.}$$

$$c_s = 0.3 \ erg/gm\text{-}^\circ K \quad . \tag{62b}$$

(iii) The properties of the gas species

(a) Steam $m = 18$; $\gamma = 1.3$, $c_p = 0.6 \ \frac{erg}{gm - {}^\circ K}$

$$\mu = 4 \times 10^{-4} \text{ poise} , \quad b = 7.34 \times 10^{-7} \ \frac{cm}{sec.} \tag{62c}$$

(b) Hydrogen gas

$$m = 2 , \quad \gamma = 1.4 , \quad c_p = 3.5 \ \frac{erg}{gm - {}^\circ K}$$

$$\mu = 2.6 \times 10^{-4} \text{ poise} \quad b = 1.25 \times 10^{-7} \text{ cm/sec.} \quad . \tag{62d}$$

The choice of the value of $\bar{b}$ for for different gas species will be discussed in part (c) of this section. It should be noted that the value

of b used here is different from that used by O'Keefe and Adams[5], which is $b = 3.56 \times 10^{-7}$ for steam. But our values of b are of the same order of magnitude. The difference is due to the different definition of Jeffreys number. We both used the condition $J_e/37.5 = 1$ in the terrestrial case to determine the value of b.

We present our numerical results in three parts: (a) isothermal ash flow, (b) ash flow with heat transfer and (c) the effect of different gas species as follows:

(a) Isothermal ash flow. We have made systematical calculations for two cases of isothermal ash flow:

(i) In the first case, we consider $\bar{u}_o = 0$ and let $(J_e/37.5)$ various from 0.01 to 5.0. The terrestrial case corresponds to $(J_e/37.5) = 1$, while the lunar case corresponds to $(J_e/37.5) = 0.028$. In our calculations, we keep ρ_{sp} and T_o unchanged and assume that the total mass of ash per square centimeter remains the same whether it is on earth, or on moon or on other planet. As a result, we have

$$\frac{G_1}{G_2} = \frac{(\rho_{go})_2}{(\rho_{go})_1} = \frac{(p_o)_2}{(p_o)_1} = \frac{g_2}{g_1} = \left(\frac{J_{e2}}{J_{e1}}\right)^{1/2} \tag{63}$$

where subscript 1 and 2 refer to the values of two different planets, e.g., one may be the earth while the other may be the moon or other planet. In our calculations, for given values of J_{e1} and J_{e2}, we have definite values for G_1/G_2.

(ii) In the second case, we consider a series values of $\bar{u}_o$, which is assumed to be of the order of $1/G$, for the lunar case only i.e., $J_e/37.5 = 0.028$ and $G = 21200$ where the gas is assumed to be steam.

The numerical results for isothermal ash flow with steam as the gas are presented in figures 4 - 11.

In Fig. 4, we plot $\bar{p}$ as a function of altitude $\bar{y}$ for various values of J_e for the case of $\bar{u}_o = 0$. In this report, altitude refers to the height from the top of the fixed bed (Fig. 1). Each curve for a given J_e starts with a triangle which marks the point of minimum fluidization, i.e., $Z = 0.4$. From there on the continuum theory of the two phase flow begins to be valid. The actual results for the pressure are given by the solid curves. If we neglect the weight of the gas entirely, the pressure curves would be those given by the dotted curves. Thus we see that the weight of the gas is responsible for the pressure drop in the dilute phase region. Hence O'Keefe and Adams[5] in which they neglected the effect of weight of gas hold true in the dense phase only. From Fig. 4, the following conclusions may be drawn:

(1) For small values of J_e, such as the case on the moon, the pressure drop takes place mostly in the dilute phase region. This indicates the importance of the dilute phase of lunar ash flow as compared to its counterpart on earth.

(2) In the case of the earth, on the other hand, the weight of the gas is relatively unimportant in its effects on pressure drop for large values of J_e. Thus the dilute phase is not important in terrestrial ash flow.

Fig. 5 shows the pressure-altitude relations on the moon for various values of initial velocity $\bar{u}_o$. We assume that

$$\bar{u}_o = \frac{N}{G} \tag{64}$$

where N is constant. We calculate the cases for N = $\frac{1}{2}$, 1, 2, 4, 8, and 16. The results show that the larger the initial velocity $\bar{u}_o$, the faster the pressure drop will be as the altitude increases when all the other parameters remain unchanged.

Figure 6 shows the velocity of the gas $\bar{u}_g$ as a function of the altitude $\bar{y}$ for the case $\bar{u}_o = 0$, i.e., $\bar{u}_p \equiv 0$, at various values of J_e.

In Fig. 7. we plot both the velocity of the particles $\bar{u}_p$ (dotted curves) and that of the gas (solid curves) against the altitude $\bar{y}$ at various values of $\bar{u}_o$ (i.e., various values of N), for the lunar ash flow. It is interesting to notice that for small values of $\bar{u}_o$ (say $N < 0.5$)the particles will not move beyond a certain altitude even though an initial velocity of the particles is assumed. For $N \geq 1$, $\bar{u}_p$ will always increase with the altitude $\bar{y}$. In low altitude, the velocity of solid particles $\bar{u}_p$ is always smaller than that of the gas $\bar{u}_g$. But at high altitudes, the difference between $\bar{u}_p$ and $\bar{u}_g$ can hardly be distinguished. This means that as the flow of the mixture goes on, the flow field will finally reach its equilibrium condition in which the velocity of the particles is equal to that of the gas. This phenomenon is the well known pneumatic transportation of small particles.

Figure 8 gives the values of volume fraction of solid particles Z as a function of altitude $\bar{y}$ at various values of J_e for the case of $\bar{u}_o = 0$ while Fig. 9 gives the values of Z as a function of altitude $\bar{y}$ at various values of initial velocity $\bar{u}_o$(or N) on the moon. It is interesting to note that even though the spread of ash over the altitude is broader for small value of J_e in the Z range calculated, yet for Z = 0.1, the larger the value J_e is, the larger is the corresponding $\bar{y}$. Hence more ash is concentrated in low altitude for smaller values of J_e than that for larger value of J_e.

It should be noticed that for values of Z less than 10^{-5}, the particles per unit cubic centimeter is so small that the accuracy

of the theory of continuum may not be good. On the other hand, we may not be interested in such small values of Z for lunar ash flow. We include the value of Z less than 10^{-8} for future reference.

We are interested in local scale height of lunar ash flow. The local scale height for atmoshpere with gas only may be defined by the following relation:

$$\frac{dp}{p} = -\frac{dy}{RT/mg} = -\frac{dy}{H_S} \tag{65}$$

where

$$H_S = \frac{RT}{mg} = \text{local scale height} \quad . \tag{66}$$

In general the temperature T varies with altitude and thus the local scale height H_S varies with altitude. But for an isothermal atmoshpere, the local scale height is a constant for all altitude. It represents the difference in altitude in which the pressure drops to $1/e$ of its original value where e is the base of natural logarithm.

In the case of the isothermal ash flow, we should modify Eqs. (65) and (66) for the mixture of the gas and solid particles. In other words, we have to use an effective molecular weight m_M instead of the true molecular weight m of the gas in the determination of scale height. From Eq. (5), if the inertial terms are negligible, we have

$$\frac{dp}{p} = -\frac{dy}{\{[(1-Z)\rho_g + Z\rho_{sp}]g\}^{-1}p} = -\frac{dy}{\frac{RT}{mg}\left[(1-Z) + Z\frac{\rho_{sp}}{\rho_g}\right]^{-1}} = -\frac{dy}{H_{SM}} \tag{67}$$

where

$$H_{SM} = \frac{\frac{RT}{mg}}{\left[(1 - Z) + Z\frac{\rho_{sp}}{\rho_g}\right]} = \text{local scale height of the ash flow} \quad . \tag{68}$$

The interesting point is that for the ash flow, the local scale height H_{SM} is not a constant for the isothermal case because of the variation of the volume fraction of solid particles with the altitude. Eqs. (67) and (68) in non-dimensional form are respectively as follows:

$$\frac{d\bar{p}}{\bar{p}} = -\frac{d\bar{y}}{\bar{p}G[(1 - Z)\bar{\rho}_g + ZG]^{-1}} = -\frac{d\bar{y}}{H^*_{SM}G} = -\frac{d\bar{y}}{H_{SM}} \tag{69}$$

and

$$H^*_{SM} = \frac{H_{SM}}{RT/mg} = \frac{\bar{p}}{(1 - Z)\bar{\rho}_g + ZG} = \frac{\bar{p}}{(1 - Z)\bar{p} + ZG} \tag{7}$$

where for convenience, we write the non-dimensional local scale height $\bar{H}_{SM} = H_{SM}/L = H^*_{SM}G$.

In Fig. 10, we plot H^*_{SM} as $\bar{y}$ for the lunar ash flow of our numerical example at various values of N . Since H_{SM} is not a constant, it would be preferable to use an average scale height H_{Sa} through which the pressure drops to $1/e$ of its original value at $\bar{y} = 0$ for isothermal lunar ash flow. Such an average scale height may be determined from the pressure curves of Figs.4 and 5 and is shown in Fig.11 as a function for J_e for the case $\bar{u}_o = 0$.

The local scale height of isothermal ash flow increases with altitude but its rate of increase decreases as the initial velocity of the particles increases. The average scale height of lunar ash is much larger than that of terrestrial ash.

(b) <u>The effects of heat transfer.</u> There are three different heat transfer processes in the ash flow which are (i) the heat convection of the mixture of the gas and solid particles (ii) the heat conduction of the mixture of the gas and solid particles and (iii) the heat transfer

between the gas and the solid particles. As we have mentioned in section II, the heat conduction of the mixture is negligible if we do not consider the transition or boundary layer region near a solid boundary. In our problems, we have neglected the heat conduction of the ash flow. From our discussion in section IV , since the parameters $27/4\ G/P_r J_e H$ is a very large number , we conclude, that the heat transfer between the gas and the ash is so rapid that these two species are in local thermal equilibrium everywhere throughout the flow field. Thus in studying the effects of heat transfer, we need to consider the temperature distribution of the mixture of the gas and the ash $\bar{T}$ through the heat convection process, Eq. (51) only. With heat transfer, we should use Eq. (15) to determine $\bar{\rho}_g$ from $\bar{p}$ and $\bar{T}$. We have carried out the numerical integration discussed in section IV (b) for the case with heat transfer to obtain the unknowns from the beginning of minimum fluidization level. The numerical method used is a fourth order Runge-Kutta method (the same method was used in the isothermal ash flow). These numerical solutions have been checked with the analytic solution in the dense phase region with heat transfer effects. Our numerical results are mainly for the lunar ash flows with heat transfer except a few cases for earth in order to compare the difference of the effects of heat transfer between moon and earth. The results are given in Figs. 12 to 20 in which the gas is steam. Since in our isothermal ash flow results the gas is steam, we may compare the ash flow with heat transfer to the corresponding isothermal ash flow.

Figure 12 shows the pressure distribution as a function of altitude at various values of $\bar{u}_o$ on the moon with heat transfer. We should compare the results of Fig. 12 to those of Fig. 5. For $N > 1$, the pressure distributions with and without heat transfer are qualitatively the same such that, as N decreases, the rate of pressure drop decreases too. But

for $N < 1$, the effect of heat transfer has a great influence on the pressure distribution. For $N < 1$, the rate of pressure drop increases enormously as N decreases and the pressure drops very rapidly as $N \to 0$. Hence for $N < 1$, the pressure distributions with heat transfer differ greatly from those of isothermal case.

Figure 13 shows the distribution of the density of gas as a function of altitude. With heat transfer, the distribution density $\bar{\rho}_g$ is different from that of pressure $\bar{p}$ while in the isothermal case, we have $\bar{\rho}_g = \bar{p}$. It is interesting to notice that with heat transfer, the density of gas may increase to 20 times of its original value for $\bar{u}_o = 0$ case and drops rapidly from this maximum value. The large variation of gas density makes the pressure distribution different from that of isothermal case.

Figure 14 shows the temperature distributions at various $\bar{u}_o$ on the moon. For $N \gtrsim 8$, the temperature variation is small in the most part of the flow field, which suggests that the isothermal approximation is a good one for these lunar ash flows. For small values of N, particularly $N \to 0$, the variation of temperature in the flow field is large. Hence the isothermal approximation is not a good one for small N, particularly $N \to 0$.

In Figure 15, the distributions of velocities of gas and solid particles are plotted as functions of altitude at various values of $\bar{u}_o$. We find that for cases of $N \lesssim 1$, the velocity of solid particles becomes zero at certain level y_c while in isothermal cases, this occurs at $N \lesssim 0.5$. Otherwise, the general trend of velocity distributions of gas and solid particles is similar for the cases with and without heat transfer. Usually, heat transfer has little influence on velocity distribution.

In Figure 16, we plot the distribution of volume fraction of solid particles as functions of altitude at various values of $\bar{u}_o$. It is seen that for $N < 0.5$, the range of dense phase $(Z \geqslant 0.2)$ increases rapidly as N decreases. We do not have similar situation in isothermal case. It is also interesting to notice the rapid drop in volume fraction of solid particles after the dense phase at small values of $\bar{u}_o$ for the case with heat transfer.

Figure 12 to 16 give mainly the results of lunar ash flow with heat transfer. We also make some numerical calculations for the comparison between the flow field with and without heat transfer on the moon with those on the earth for two typical values of initial velocity, i.e., $N = 0$ and 8 as follows:

Figure 17 shows the comparison of pressure distribution at $\bar{u}_o = 0$ or $N = 0$. Tremendous change of pressure distribution is shown on the moon due to the influence of heat transfer while on earth the effect of heat transfer is not so significant. It is interesting to notice that in this case $(N = 0)$ with heat transfer, the pressure distributions as functions of altitude on the moon and on the earth do not differ greatly as those are in the isothermal cases.

Figure 18 shows the comparison of temperature and gas density distributions with and without heat transfer on the moon and on the earth for the case $\bar{u}_o = 0$. The distributions of gas density on the moon with and without heat transfer bear no similarity at all while those on the earth do roughly have similar behavior. The temperature drop on the moon is much faster than that on the earth as shown in Fig. 18. As a result, the layer of hot ash is thicker on the earth than that on the moon for $\bar{u}_o = 0$.

Figure 19 shows the comparison of gas velocity and volume fraction

of solid particles at $\bar{u}_o = 0$ for those on the moon to those on the earth. Again, the effects of heat transfer are much more significant on the moon than those on the earth. The thickness of dense phase increases by 14 times due to the effect of heat transfer on the moon at $\bar{u}_o = 0$, i.e., 3 m ($\bar{y} = 0.2$, $Z = 0.2$) in isothermal case and 40 m ($\bar{y} = 2.7$, $Z = 0.2$) with heat transfer. On the other hand, the corresponding values for the thickness of dense phase on earth are 28.5 m for isothermal case, (Ref. 5 gives 30 m) and 34 m for case with heat transfer, thus we have only an increase of 1.2 times due to heat transfer.

In Fig. 20, comparison of pressure, gas density and temperature for $\bar{u}_o = 8/G$, i.e., $N = 8$, are shown. It is seen that for large N, the effect of heat transfer is small on the distributions of pressure and gas density because the temperature variations for large N is rather small and we do not have such a large drop in temperature for $N = 8$ as in the case of $N = 0$. For $N = 8$, we also find that the effects of heat transfer on gas velocity and volume fraction of solid particles are insignificant. Hence we do not show these variations. In conclusion, for large initial velocity, $\bar{u}_o \gtrsim 8/G$ or $N \gtrsim 8$, the effects of heat transfer are small and the isothermal approximation is good. And for small initial velocity $N \lesssim 8$, the effects of heat transfer become important particularly when $N \to 0$. The effect of heat transfer at small initial velocity ($N \to 0$) is to make the whole layer of ash flow more compact together on the moon. The thickness of dense phase is increased considerably by the influence of heat transfer while that of dilute phase is reduced. The direct consequences of the slow change of volume fraction of solid particles over the layer of dense phase on the moon for $N \to 0$ are that

(1) the pressure drop in the dense phase layer increases

(2) the gas density also increases and

(3) a steep vertical temperature gradient occurs.

(b) The effects of different gas species. For small values of N or $\bar{u}_o$, the flux of energy of gas is relatively large in comparison with that of pseudo-fluid of solid particles while for large values of N or $\bar{u}_o$, the flux of energy of gas is relatively small in comparison with that of pseudo-fluid of solid particles. Since gas is a compressible fluid, the effect of heat transfer on gas is large. On the other hand, the pseudo-fluid of solid particles behaves as an incompressible fluid and thus the effect of heat transfer on the solid particles is small. As a result, we see in the last part of this section that the effect of heat transfer is large for small N while it is small for large N.

Since different gas has different specific heat or different heat capacity, the influence of heat transfer may be different for different gases. It is interesting to investigate how large would be the effects of heat transfer on ash flow for different kinds of gas species. In our previous numerical calculations, we considered only the case in which the gas is steam. Another possible gas in an ash flow is hydrogen. Since the heat capacity of hydrogen is about six time larger than that of steam, we may find out the main influence due to different gas species by carrying out some of our numerical calculation of ash flow with hydrogen as the gas instead of the steam.

Before we make the specific numerical calculation, it would be useful if we consider the general effect on the ash flow due to the physical properties of its gas species. The physical properties of the gas species which have some influence on the ash flow are (i) the ratio of specific

heats γ , (ii) the specific heat at constant pressure c_p , (iii) the mass of a molcule of the gas m , (iv) the coefficient of viscosity μ and (v) the rate of emission of gas from the solid particles b . Among these five physical quantities, γ , c_p , m , μ , and b , only the value of b is not known very well. In order to compare the effects of the physical properties of different gas species, we have to set a criterion for this comparison. Since in our study we find that the Jeffreys number J_e , Eq. (24), is the most important parameter in the ash flow, we shall assume that the Jeffreys number J_e remains unchanged for different gas species when the other physical quantities remain unchanged. In other words, we may use the condition that $J_e = 37.5$ on earth to determine the values of b for different gas species. When the properties of solid particles, the gravitational acceleration and the initial temperature are the same, for a constant Jeffreys number, Eq. (24) gives

$$\frac{m}{\mu b} = \text{constant for any gas} = \frac{m_1}{\mu_1 b_1} = \frac{m_2}{\mu_2 b_2} \tag{71}$$

where subscripts 1 and 2 denote the values for gases 1 and 2 respectively. Thus in Eqs. (62), we have $b = 7.34 \times 10^{-7}$ cm/sec. for steam and $b = 1.25 \times 10^{-7}$ cm/sec. for hydrogen.

From Eqs. (14), (27), (28), and (30) we have the following relations for the two different kinds of gas:

$$\frac{V_{c1}}{V_{c2}} = \frac{\mu_2}{\mu_1} \; ; \quad \frac{G_1}{G_2} = \frac{m_2}{m_1} \; , \quad \frac{H_1}{H_2} = \frac{\mu_2^2}{\mu_1^2} \; , \quad \frac{\delta_1}{\delta_2} = \frac{c_{p2}}{c_{p1}} \quad . \tag{72}$$

Hence when we change the gas 1 in the ash flow to gas 2 , we have to modify the reference velocity V_c , the density ratio G , the specific heat ratio δ and the dynamic pressure parameter H in addition to the

gas property parameter γ .

Since in our investigations, we consider the case of $H \cong 0$ only, for the isothermal ash flow we need to modify the density ratio G only. When the gas is hydrogen, from Eq. (72), we have

$$G_{hydrogen} = 9\, G_{steam} \tag{73}$$

because $m_2 = 18$ for steam and $m_1 = 2$ for hydrogen. From our previous discussion of isothermal ash flow results in (a) of this section, i.e., Fig. 4, the effect of G or the relative importance of the weight of gas becomes significant only in the dilute phase or small value of Z . Thus for hydrogen, we have a larger value of G than that for steam, which implies that the effect of G comes at even smaller value of Z than those shown in Fig. 4 for the case of steam. Since the isothermal approximation is poor for small values of $\bar{u}_o$ and an increase of G would influence the results at small Z region only, the change in parameter G alone would not give much new and interesting results for the isothermal ash flow. Hence we feel that we need not study the results for isothermal ash flow with hydrogen in detail.

On the other hand, the value of c_p for hydrogen is about six times greater than that of steam, we expect that some significant effects due to the change of steam to hydrogen in the ash flow with heat transfer would occur. Hence we recalculate the ash flow variable with hydrogen as the gas species for the case with heat transfer and the results are presented as follows:

Figure 21. shows the pressure distributions of the lunar ash flow with heat transfer as functions of altitude at various values of $\bar{u}_o$ or N with hydrogen as the gas species. We compare Fig. 21 with Fig. 12 which is for the case of steam. We find that there are significant differences

between these results. For the case of steam, Fig. 12, the effects of heat transfer is not important for $N \gtrsim 1$ and important for $N \lesssim 1$. For the case of hydrogen, Fig. 21, the effects of heat transfer remain significant even when N is as high as 16. Qualitatively the pressure curves for the case of hydrogen for all $N \lesssim 16$ behave similarly as those for the case of steam when $N \lesssim 1$. The reason is evident because the larger the heat capacity of a gas is, the larger would be the relative influence of the heat transfer in the mixture due to the contribution of the gas species. Thus the influence of the heat transfer would extend to larger value of $\bar{u}_o$ or N for the gas with larger heat capacity.

Figure 22 shows the temperature distributions of the lunar ash flow with heat transfer as functions of altitude at various values of $\bar{u}_o$ or N with hydrogen as the gas species. It is evident that the isothermal approximation is not good even N = 16, due to the large heat capacity of the hydrogen gas.

From the pressure and the temperature distributions, we calculate the density distributions of the gas which are given in Fig. 13 for both the steam and hydrogen.

Figure 23 shows the corresponding distributions of velocities of the gas and the solid particles for the case of hydrogen which should be compared with the corresponding curves for the case of steam in Fig. 15. Figure 24 shows the corresponding distribution of volume fraction for the case of hydrogen gas which should be compared with Fig. 16 of the case of steam. It is evident that as long as the heat transfer effects are important, the variations of the corresponding variables are similar. In other words, the curves of hydrogen gas for $N \lesssim 16$ are similar to those of steam for $N \lesssim 1$.

VI. SUMMARY AND CONCLUSIONS

From our theoretical study and numerical results, the following conclusions may be drawn:

(1) A theoretical model of two-phase flow of a mixture of gas and small solid particles is used in studying one dimensional steady ash flows for both the lunar and terrestrial case, with special emphasis on the lunar case. The fundamental equations and the boundary conditions are described. In general, there are seven unknowns: the temperature of the gas T_g, the temperature of the solid particles T_p, the velocity of the gas u_g, the velocity of the solid particles u_p, the pressure of the mixture p, the density of the gas ρ_g and the volume fraction of the solid particles Z. For the ash flow under consideration, the temperature field is in local thermodynamic equilibrium so that $T_p = T_g = T$. We have to study six unknowns: T, p, ρ_g, u_p, u_g and Z only.

(2) From the fundamental equations and the boundary conditions of one dimensional steady ash flow, we find that there are seven non-dimensional parameters which govern the ash flow and which are: (i) Jeffreys number, Eq. (24) which is one of the most important parameters in ash flow and which represents the ratio of gravitational force to viscous force, (ii) the density ratio G, Eq. (27), which represents the effect of the weight of gas in the ash flow (iii) the dynamic pressure parameter H, Eq. (28), which represents the inertial effects in the ash flow, (iv) the initial velocity ratio $\bar{u}_o$, Eq. (23), which represents the effects of initial velocity u_o of ash relative to the characteristic velocity of emission V_c, Eq. (14), from the solid particles in the ash flow, (v) the gas property parameter γ, Eq. (29), which is the ratio of specific heat of the gas at constant pressure c_p to that at constant volume c_v, (vi) the specific heat ratio δ, Eq. (30), which is the ratio of the specific heat of the solid particles c_s to that of the gas at constant pressure

c_p , and (vii) the Prandtl number P_r , Eq. (31) which is important in the study of heat conduction in the mixture and heat transfer between species. In our study, we consider the cases where the inertial effects are negligibly small and the species in the mixture are in local thermodynamic equilibrium. Hence the parameters H and P_r will be dropped out in our analysis. We study mainly the influence of the five parameters J_e, G, $\bar{u}_o$, γ and δ .

(3) Analytical solutions to the fundamental equations with and without heat transfer have been obtained for the dense phase region of the ash flow. Numerical solutions for the whole flow field of the ash flow have been obtained for both the isothermal ash flow and the ash flow with heat transfer. In the isothermal case, the effect of different gas species is small. For the ash flow with heat transfer, the heat capacity of the gas species has a large influence on the ash flow. Hence we calculate two cases of lunar ash flow: one for steam as the gas and the other for hydrogen as the gas and compare these results. Some essential results for these cases are given below.

(4) For the isothermal ash flow, only three parameters J_e , G and $\bar{u}_o$ are important. In our calculations for isothermal ash flow, we find that the density ratio G is important only in the dilute phase where the volume fraction is very small, (see Fig. 4). Hence the change of parameter G due to the change of gas species from steam to hydrogen would change slightly the flow field in the upper dilute phase only and it would not give much new and interesting result of isothermal ash flow. Hence in our numerical solution, a major portion of the results of isothermal ash flow deals with steam only. For a definite kind of gas species, there is a definite relation between J_e and G . Hence for isothermal ash flow, the most important parameters are J_e and $\bar{u}_o$ only.

For large values of J_e, (i.e., large graviational constant if other factors remain equal), the pressure drop in the isothermal ash flow occurs mostly in the dense phase region while for small values of J_e (i.e., small gravitational constant, if other factors remain equal), the pressure p drop in the isothermal ash flow occurs mainly in the dilute phase region and for intermediate value of J_e, the pressure drop occurs in transition region as shown in Fig. 4. Hence the dilute phase region is important in the lunar ash flow.

The weight of the gas or the density ratio parameter G is much more important in the dilute phase of the isothermal ash flow than in the dense phase of the ash flow. It is responsible for the pressure drop at high altitude. Hence for the lunar ash flow, the parameter G is very important.

Since we study mainly the flow field due to the emission of gas from the ash, at small initial velocity ratio $\bar{u}_o \lesssim 0.25$, the particle velocity may become zero when the altitude is above a certain critical height because we assume that no particle (or negligible amount of particles) comes from outer space. For large values of $\bar{u}_o$ ($\bar{u}_o \gtrsim 0.5$), the velocity of the particles u_p increases with altitude y just as that of the gas u_g. At low altitude, the velocity of the particles u_p is always less than that of the gas u_g, while at high altitude, the equilibrium condition will be reached and then the velocity of the particles is nearly equal to that of the gas.

The local scale height of the isothermal ash flow increases with the altitude but its rate of increase decreases as the initial velocity of the particles increases.

(5) For the ash flow with heat transfer, we first reexamine

our isothermal results for steam with heat transfer. The most important heat transfer process in the ash flow is due to heat convection in the mixture. Our numerical results, given in Figs. 12 to 20, show that the effect of heat transfer becomes important for the cases of small initial velocity $\bar{u}_o$. For the case of steam as the gas species, the effect of heat transfer is very small if $\bar{u}_o \geq 8/G$, i.e., $N \geq 8$, but for $N < 1$ especially for $N \to 0$, the influence of heat transfer is very large. As $N \to 0$, the effect of heat transfer is to make the whole layer of ash flow more compact together on the moon. The thickness of the dense phase of lunar ash flow is increased considerably by the influence of heat transfer while that of dilute phase is reduced. The pressure drop in the dense phase layer of lunar ash increases and the gas density also increases and reaches a maximum and then reduces due to the effect of heat transfer.

(6) Since the effect of heat transfer depends greatly on the heat capacity of the gas species, we reexamine our numerical results for steam by using the hydrogen as the gas species for the lunar ash flow. Since the heat capacity of hydrogen is about 6 times that of steam, we do find that the effect of heat transfer with hydrogen is much larger than that with steam. Qualitatively, the effect of heat transfer still depends on the initial velocity $\bar{u}_o$. The larger the value $\bar{u}_o$ is, the smaller the influence of heat transfer will be if other parameter remain unchanged. But for steam, we find that when $\bar{u}_o \geq 8/G$ or $N \geq 8$, the effect of heat transfer is negligibly small. However, for hydrogen, the effect of heat transfer is not negligible even if $N = 16$.

REFERENCES

1. Pai, S.I., T. Hsieh and J.A. O'Keefe, Lunar Ash Flow: The Isothermal Approximation, to be published in J. Geophys. Res.
2. Schumm, S.A., Experimental Studies on the Formation of Lunar Surface Features by Fluidization. Geological Society of American Bulletin, vol. 81, Sept. 1970, pp. 2539-2552.
3. Pai, S.I., A Review of Fundamental Equations of the Mixture of a Gas with Small Solid Particles, Tech. Note BN-668, IFDAM, University of Maryland, 1970.
4. Anderson, A.G., Sedimentation, Section 18. Handbook of Fluid Dynamics, Ed. by V.L. Streeter, McGraw-Hill Book Co., Inc. 1961.
5. O'Keefe, J.A. and E.W. Adams, Tektite Structure and Lunar Ash Flows, J. Geophys. Res. vol. 70, No. 16, Aug. 1965, pp. 3819-3829.
6. Happel, J., Viscous Flow in Multiparticle Systems: Slow Motion of Fluids Relative to Beds of Spherical Particles, A.I. Ch.E. Journ., Vol. 4, No. 2, 1958, pp. 197-201.
7. Kuwabara, S., The Forces Experienced by Randomly Distributed Parallel Circular Cylinders or Spheres in a Viscous Flow at Small Reynolds Numbers, J. of Phys. Soc. of Japan, Vol. 14, No. 4, 1959, pp. 527-532.
8. Ergun, S., Fluid Flow Through Packed Columns, Chem. Engr. Prog, Vol. 48, No. 2, Feb. 1952, pp. 89-94.
9. Leva, M., Fluidization, McGraw-Hill Book Co., N.Y., 1959.
10. Rowe, P.N., Drag Forces in a Hydraulic Model of a Fluidized Bed, Part II, Trans. Inst. Chem. Engr. Vol. 39, 1961, pp. 175-180.
11. O'Keefe, J.A. Water on the Moon and a New Non-Dimensional Number, Science, Vol. 163, Febr., 1969, pp. 669-670.

APPENDIX I

ON THE PRESSURE GRADIENT IN FLUID-SOLID TWO-PHASE FLOW AT LOW REYNOLDS NUMBER

Introduction

One of the main difficulties in the application of equations of motion of a mixture of fluid and small solid particles is the correct expression for the interaction forces between the fluid and the solid particles. Generally, the interaction forces depend on the Reynolds number, Mach number, Knudsen number, shape, size, surface condition, number density and rotation of the particles as well as the interaction between particles in the local flow field (1'and references thereon). However, in most engineering problems, we usually assume that the particles may be represented by uniform spheres with an effective radius r_p and the Reynolds number of the particles, $R_e = 2\rho_f U r_p/\mu$, is the dominant factor. The other effects may be important only at particular situations. Therefore, the interaction force term which appears in the momentum equation of two-phase flow may be represented by the viscous drag force of spheres in a uniform flow as a first approximation. Even after such a simplification, it is not straightforward to write down the interaction force term because the viscous drag force of many spheres in a uniform stream is still lacking. Single sphere in infinite domain at low Reynolds number ($R_e < 0.1$) the viscous drag force is given by Stokes' law, or Oseen's approximation at $R_e \sim 1$; while at high Reynolds number only empirical curve is available. With the presence of many spheres in a finite domain, even at low Reynolds number, we have to rely on experimental information for the drag force. Thus, it is quite frequent that

an empirical equation for the pressure gradient is used in the calculation of fluid-solid two-phase flow at low Reynolds number, where the inertial terms are negligible (2', 3', 4' and 5'). Empirical equations of pressure gradient for spheres in a finite domain have been reported by many authors (2', 3' and references thereon), however, due to the empirical nature of these equations, their applications are restricted to some range of the volume fraction of the solid particles (a typical parameter to be used) or concentration. It is the purpose of this note to present a useful equation for the pressure gradient which covers the entire range of the volume fraction of the solid particles of practical interest ($0 < Z \lesssim 0.4$) for fluidized bed and fits well to most of the available experimental data at low Reynolds number flow.

Experimental Results

A general form of the available empirical equation for pressure gradient of fluid flow through packed columns due to the viscous energy dissipation alone at high concentration may be expressed as follows:

$$\frac{dp}{dy} = -\frac{K\mu}{r_p^2} \cdot \frac{Z^2}{(1-Z)^3} U_m = -\frac{K\mu}{r_p^2} \cdot \frac{Z^2}{(1-Z)^2} u_f \qquad (1')$$

where

$$U_m = (1-Z)u_f \quad . \qquad (2')$$

The constant K is 45 in Carman-Kozeny's equation with $k = 5$(6') and is 37.5 in Ergun's equation (2') and 50 in Leva's equation (3') for spherical particles (in fact, K is between 36 and 50 as reported by different experimentors (3')). Equation (1') is valid for laminar flow and is restricted to $Z > 0.2$.

Rowe (7') expressed his experimental results for the drag force of a single sphere at the presence of other equally spaced spheres as follows:

$$F_s = C_D(\pi r_p^2)\ \frac{1}{2}\rho_f\ U_m^2\ (1 + \frac{0.68}{h/r_p}) \tag{3'}$$

where

$$C_D = \frac{24}{R_e}\ (1 + 0.15\ R_e^{0.687}) \tag{4'}$$

and $R_e = 2r_p\rho_f U_m/\mu$. At low Reynolds number ($R_e < 1$) , the second term in the parenthesis may be dropped. As shown in the Appendix II, h/r_p may be expressed by Z as

$$\frac{h}{r_p} = (1.35Z)^{-\frac{1}{3}} - 1 \tag{5'}$$

for rhombohedral packing. Since

$$Z = n\ (\frac{4}{3}\pi\ r_p^3) \tag{6'}$$

where n is the number density of the spheres per unit volume, the total drag force per unit volume becomes

$$F_p = nF_s = \frac{9Z\mu}{2r_p^2}\ U_m\ (1 + \frac{0.68}{h/r_p})\ . \tag{7'}$$

Rowe performed his experiment at $R_e = 32$ to 96 and $h/r_p = .1$ to 1.

New Equation

In general, the minimum fluidization occurs at $Z \sim 0.4$. For a fluidized flow of mixture of fluid and small solid particles, we are interested in the range of Z from 0 to 0.4. We note that at small values of Z , the pressure drop is mainly due to the frictional drag between the fluid and the solid particles. As a result, Eq. (7') may be

interpreted as the pressure gradient at small values of Z. As $Z \to 0$, Eq. (7') may be reduced to

$$\frac{1}{n} \frac{dp}{dy} = - 6 \pi r_p \mu u_f \qquad (8')$$

which is the well-known Stokes' law for frictional drag of sphere in infinite stream at low Reynolds number. On the other hand, Eq. (7') fails to describe the pressure gradient at high concentration region of $Z > 0.2$ and at low Reynolds number (see Fig. 25). Since Eq. (7') has the correct limiting case of Stokes' law as Z approaches zero, in view of Eq. (1'), it is not difficult to realize that a term of $(1 - Z)^3$ in the denominator should help at high concentration region. By doing so, we find a new equation which gives the pressure gradient in a flow of mixture of fluid and small solid particles at low Reynold number and fits well with most available experimental data as follows:

$$\frac{dp}{dy} = - \frac{9\mu}{2r_p^2} \frac{Z}{(1 - Z)^2} \left(1 + \frac{0.68}{h/r_p}\right) u_f \quad . \qquad (9')$$

A plot of Eq. (9') is shown in Fig. 25 as a function of Z.

Comparison with Experimental and Theoretical Results

A comparison of Eq. (9') with most available experimental data is also shown in Fig. 25. At high concentration of $Z > 0.2$, Eq. (9') coincides perfectly with Carman-Kozeny equation with $k = 5$ between $Z = 0.25$ and 0.45 and falls in between that of Ergun and Leva. At intermediate concentration of Z from 0.05 to 0.2, the data of Happel and Eppstein, Steinour, Mertes and Rhodes, Hanratty and Bandukwala as reported in Ref. 6' and 8' and Adler and Happel (9') are also plotted in Fig. 25.

The large deviation among the data in this range may be due to the effects other than concentration, such as agglomeration and segregation and an oriental factor is also suggested in Ref. 9'. It seems to the author, the data of Happel and Eppstein is most reliable to show the effect of concentration since their data agree with that of Ergun within experimental error at high concentration region, $Z = 0.2$ to 0.5. Eq. (9') also represents Happel and Epstein's data to within 15 % higher. At dilute region, Eq. (9') also agrees closely with the experimental data of McNown and Lin (10') to within 10 % lower. Therefore, Eq. (9') is indeed a best fitted equation to all the experimental data available at present. Other semi-empirical equations, which only cover a small range of concentration, and do not show large difference from the data presented in Fig. 25 , may be found in Ref. 6' and references thereon and are not reported here.

The only theoretical models related to the present work are those of Happel (6') and Kuwabara (11'). Their results are also plotted in Fig. 1' with concentration defined as $Z = r_p^3/(h + r_p)^3$. It is seen that Eq. (9') fits the experimental data better than those theoretical results. Another point of the theoretical work subjected to criticism is that its definition of concentration $Z = r_p^3/(h + r_p)^3$, which is obviously impractical at high concentration region, $Z > 0.2$ say. Should Eq. (5') be used to calculate the concentration from the ratio of h/r_p , the drag would be increased by 6.3 and 4.62 times at $Z = 0.5$ and 2 and 1.53 times at $Z = 0.2$ respectively for Happel's and Kuwabara's model. For packing other than rhombohedral, the increase in drag at high concentration region would be greater. It is obvious that any theoretical model would not be satisfactory at high concentration due to the complexity of the flow. Hence, it is on the safe side to use experimental results such as Eq. (9') to carry out computation for lunar ash flow.

APPENDIX II

GEOMETRIC CONSIDERATION OF VOLUME FRACTION OF SOLID PARTICLES

Let the radius of the spheres (solid particles) be r_p and the half spacing between nearby spheres be h. To calculate the volume fraction of the solid particles, we may consider the packing of the invisible spheres of radius $h + r_p$. The closest packing of uniform spheres is the rhombohedral packing as described by Graton and Fraser (12'). As shown in Fig. 26, 14 of the invisible spheres may be put together to form a cubic of side $2\sqrt{2}(h + r_p)$ while each sphere involved has some part of its volume excluded from the cubic. Such cubic may continuously repeat itself throughout the space in our problem. The total number of spheres inside the cubic is 4. Thus, we have

$$V_c = \text{volume of the cubic} = 16\sqrt{2}\,(h + r_p)^3$$

$$V_s = \text{volume of solid particles} = 4\,\frac{4}{3}\,\pi\,r_p^3$$

and

$$Z = \frac{V_s}{V_c} = 0.74\left(\frac{h}{r_p} + 1\right)^{-3}$$

or

$$\frac{h}{r_p} = (1.35Z)^{-\frac{1}{3}} - 1$$

when $h = 0, Z = 0.74$ which is the maximum volume fraction of spheres.

REFERENCES FOR APPENDIX I AND II

1. Pai, S.I., Technical Note BN-668 IFDAM, University of Md., Aug. 1970.
2. Ergun, S., Chem. Engr. Prog., vol. 48, No. 2, pp. 89-94, Feb. 1962.
3. Leva, M., Fluidization, P. 47, McGraw-Hill, New York, 1959.
4. Stokel, I.H., Chem. Engr. Prog., vol. 58, Symp. Series 38, 1962.
5. O'Keefe, J.A. and Adams, E.W., J. of Geoph. Res., vol. 70, No. 16, Aug. 1965, pp. 3819-3829.
6. Happel, J., A. I. Ch. E. Journal, vol. 4, p. 197, (1958).
7. Rowe, P.N., Trans. Inst. Chem. Engr., vol. 39, pp. 175-180, (1961).
8. Happel, J. and Epstein, N., Ind. Eng. Chem., vol. 46, p. 1187 (1954).
9. Adler, I.L. and Happel, J., Chem. Engr. Prog., vol. 58, Symp. Series No 38, (1962).
10. McNown, J.S. and Lin, P.N., Proc. 2nd Midwestern Conf. of Fluid Mechanics, Ohio State Univ., (1952).
11. Kuwabara, S., J. Phys. Soc. Japan, vol. 14, p. 527, (1959).
12. Graton, L.C. and Fraser, H.J., J. of Geol., vol. 43, pp. 785-909, (1935).

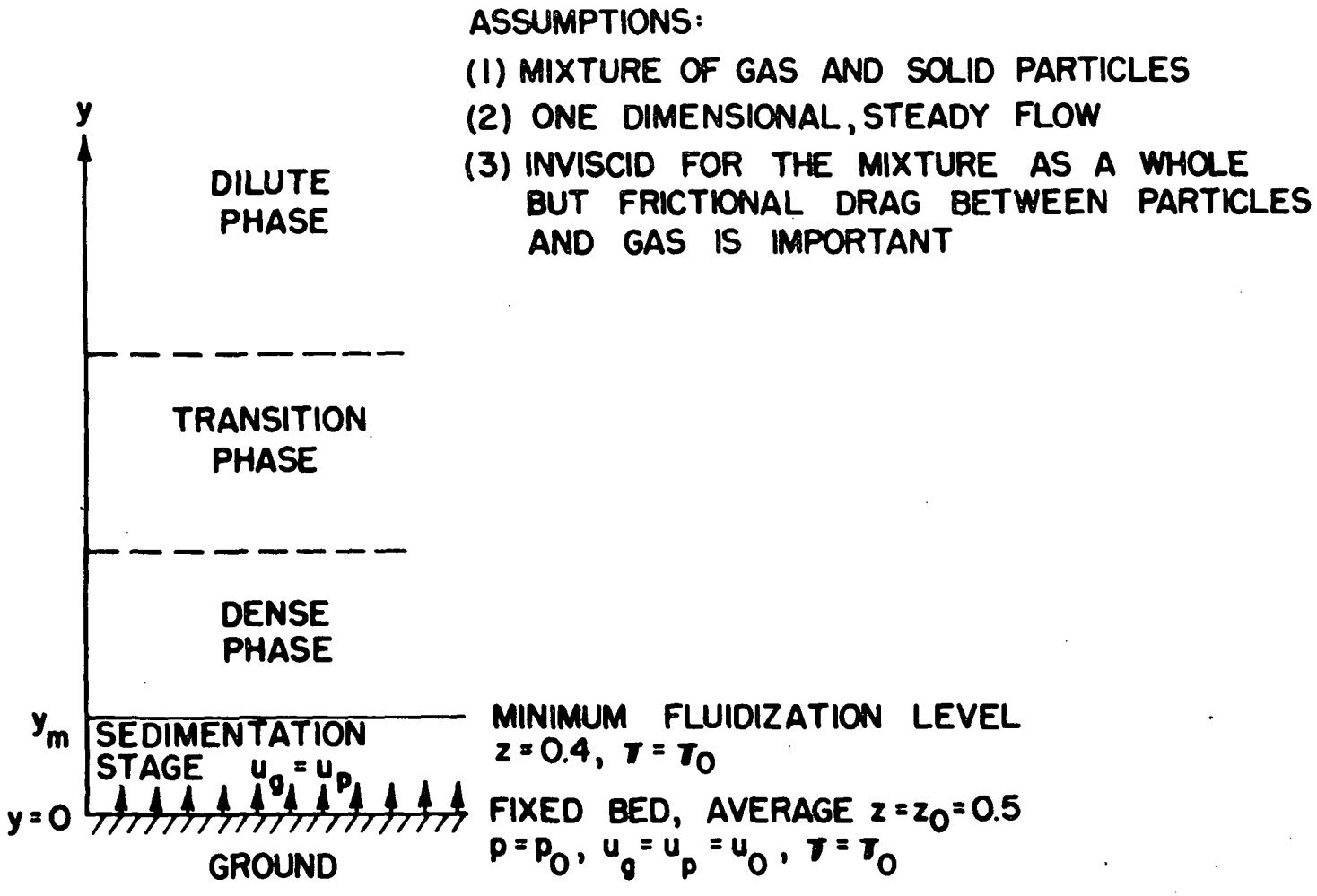

Fig. 1 SKETCH OF ASH FLOW

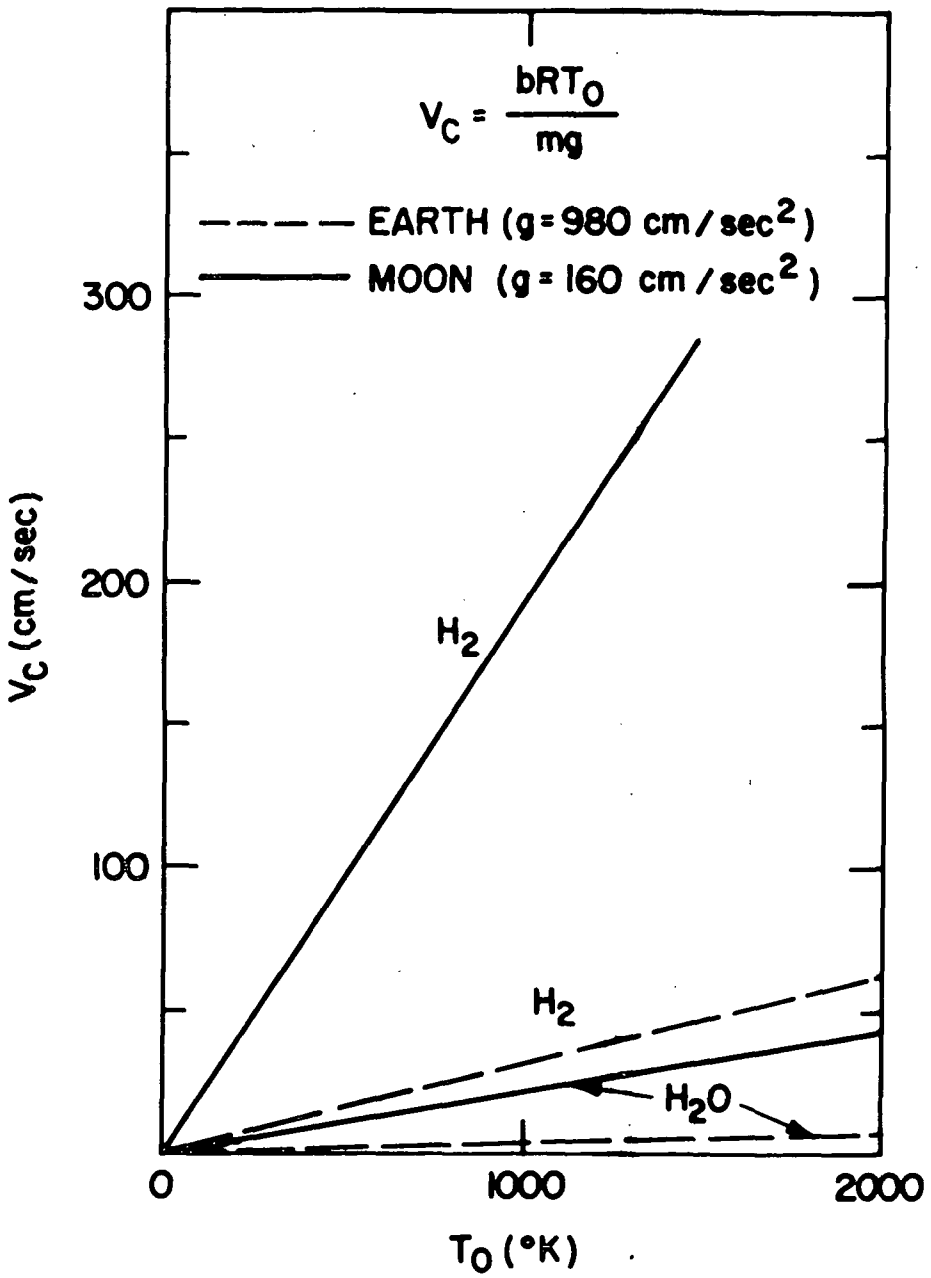

Fig. 2 CHARACTERISTIC VELOCITY v_c AS A FUNCTION OF T_o .

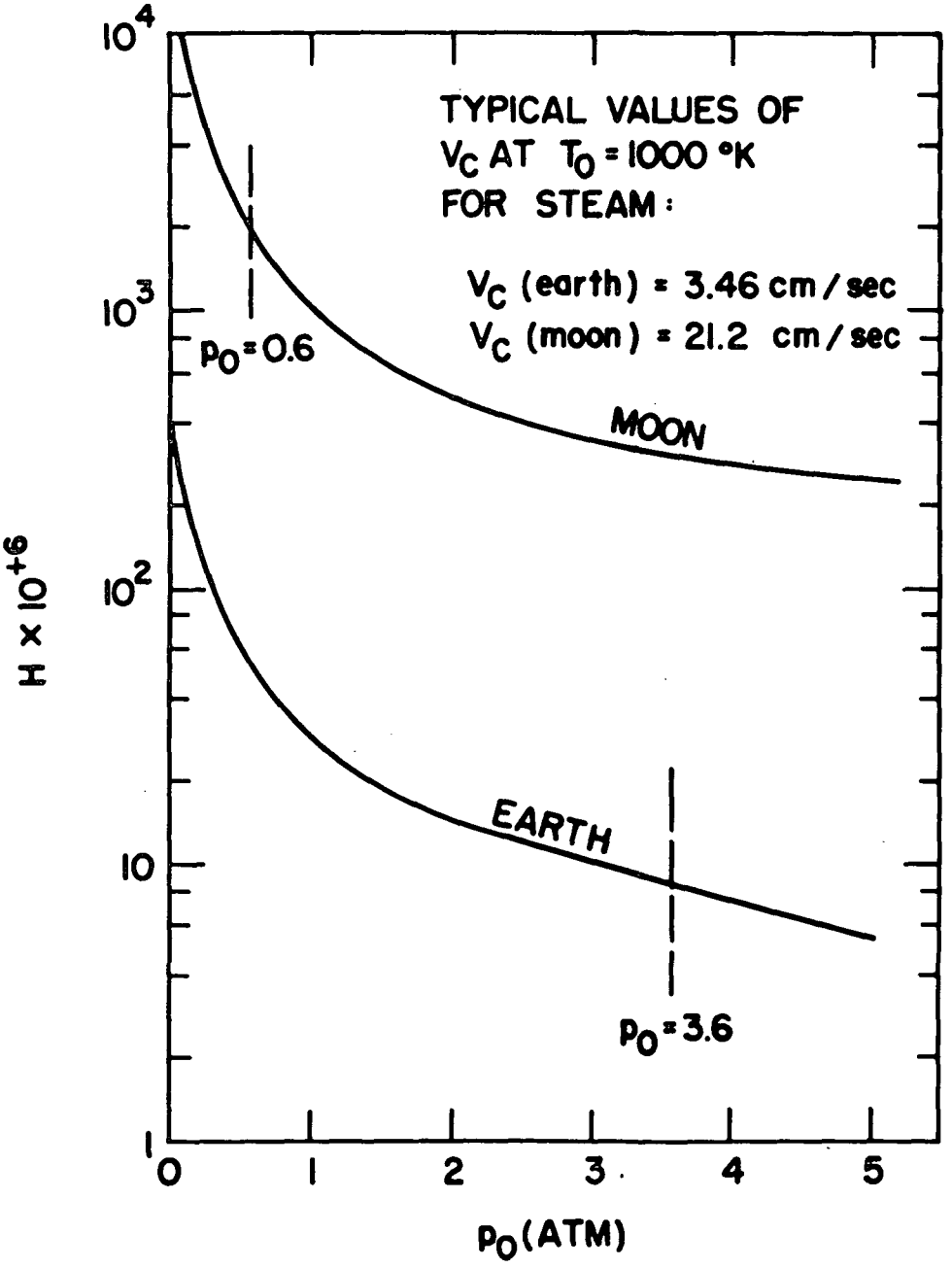

Fig. 3 DYNAMIC PRESSURE PARAMATER H

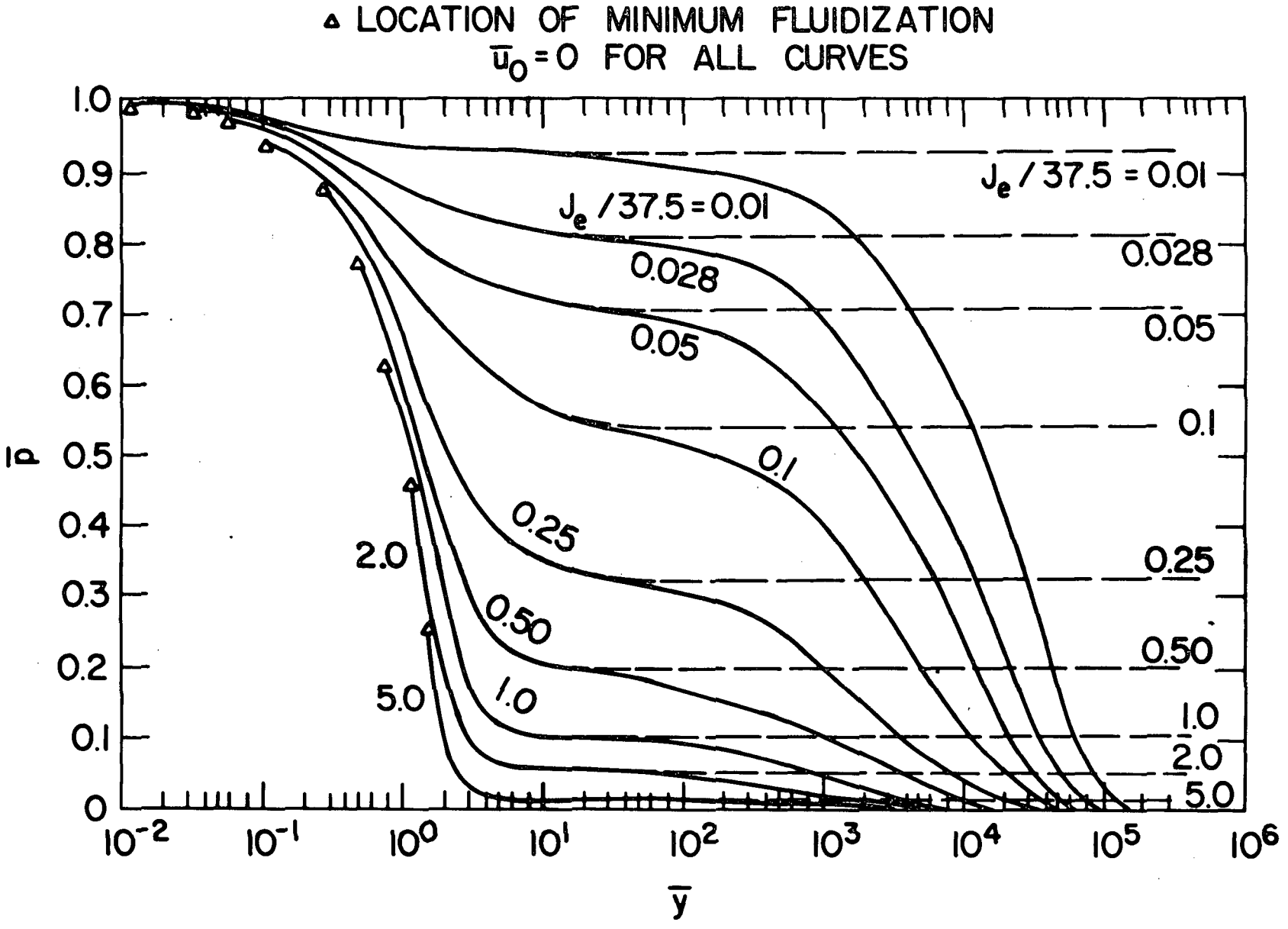

Fig. 4 $\bar{p}$ AS A FUNCTION OF ALTITUDE AT DIFFERENT VALUES OF J_e

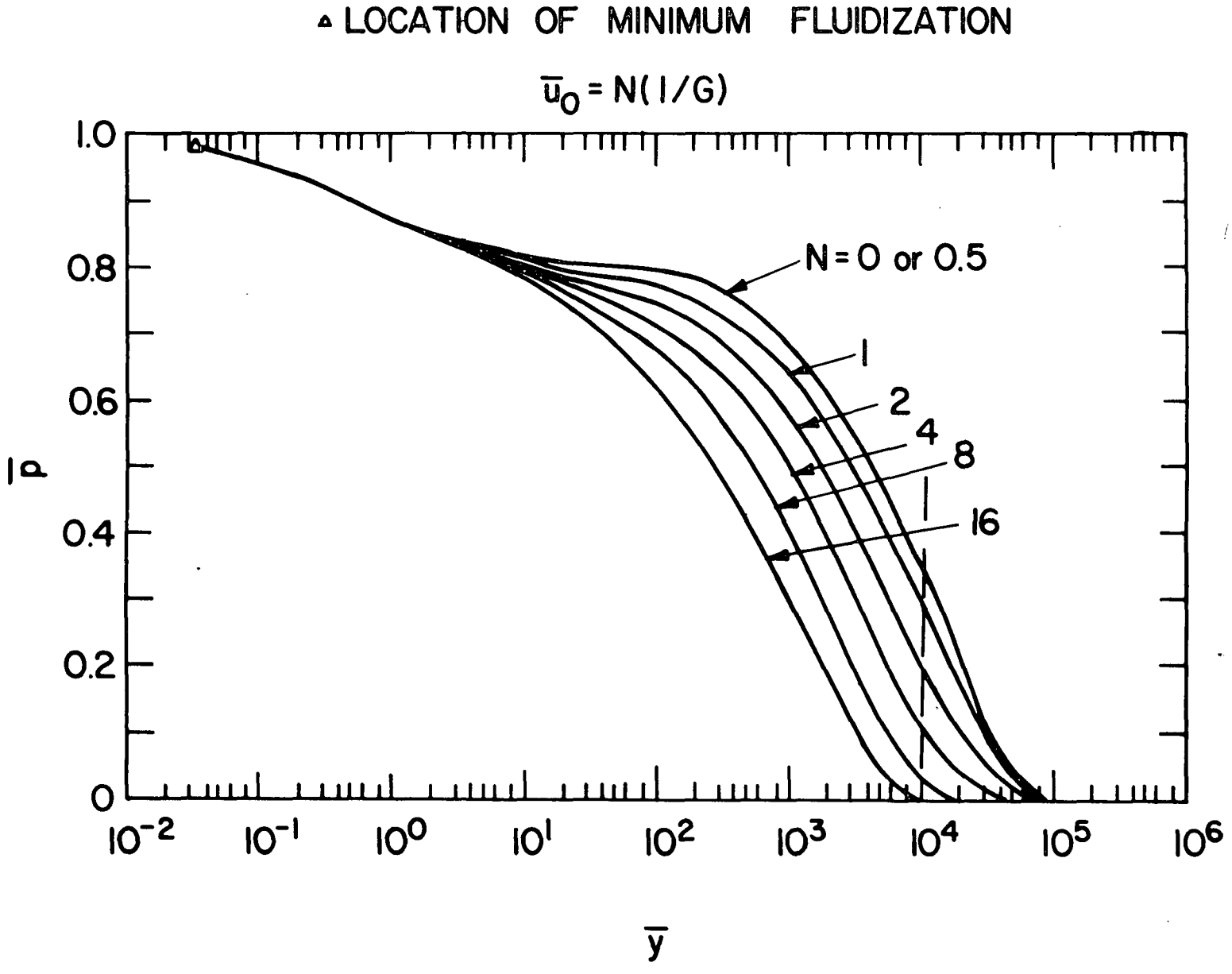

Fig. 5 $\bar{p}$ AS A FUNCTION OF ALTITUDE AT DIFFERENT VALUES OF $\bar{u}_o$

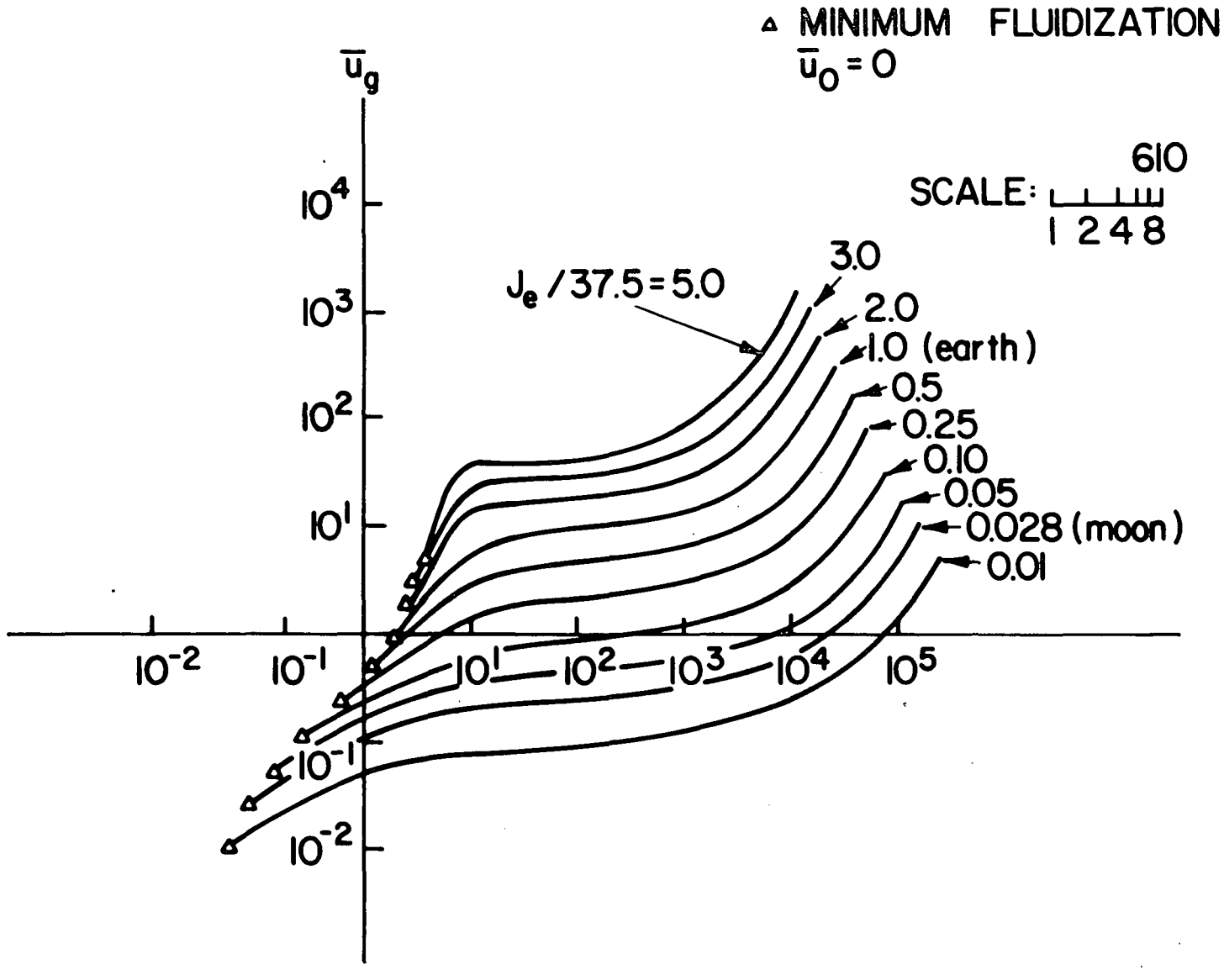

Fig. 6 $\bar{u}_g$ AS A FUNCTION OF ALTITUDE

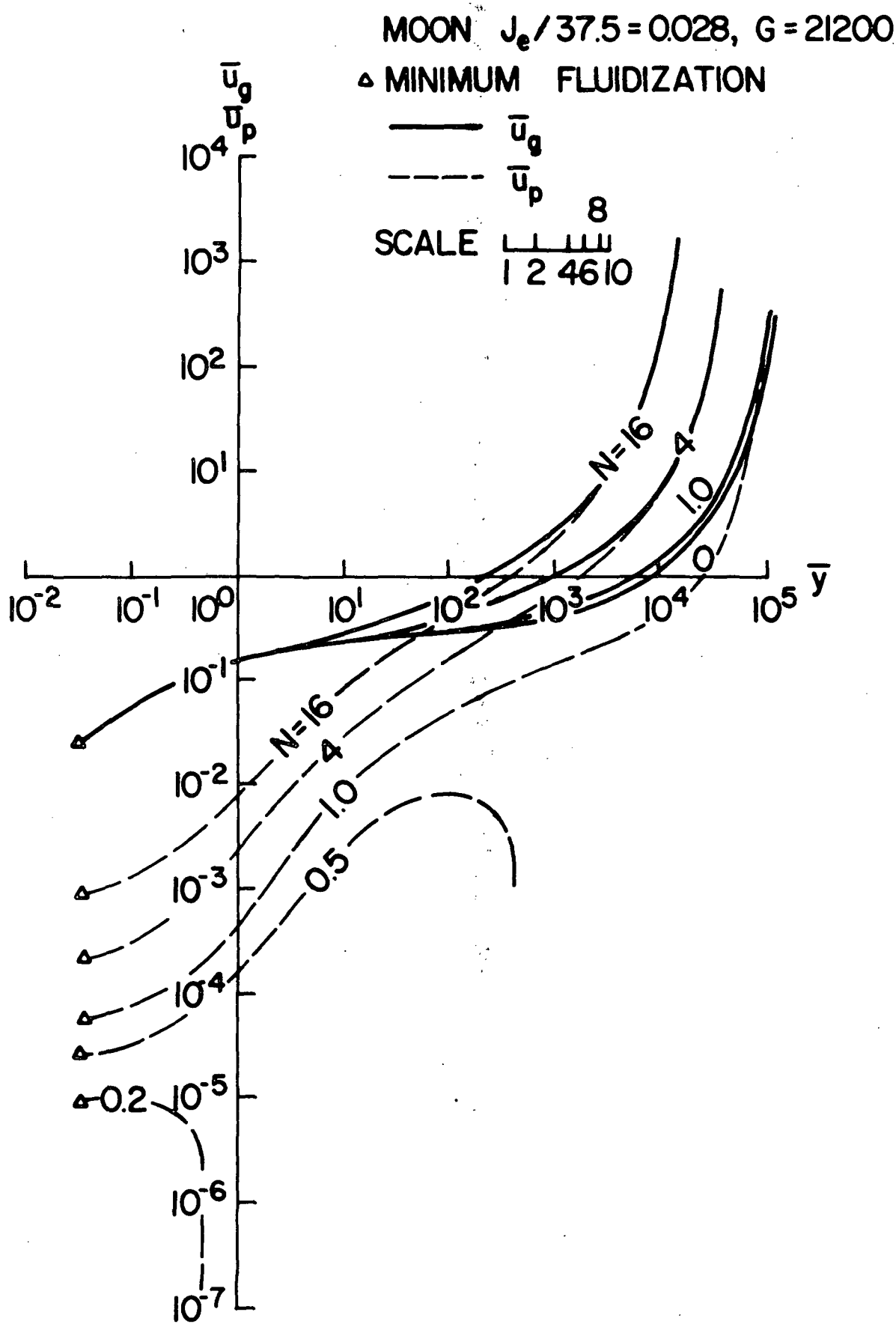

Fig. 7 $\bar{u}_g$ and $\bar{u}_p$ AS A FUNCTION OF ALTITUDE FOR MOON

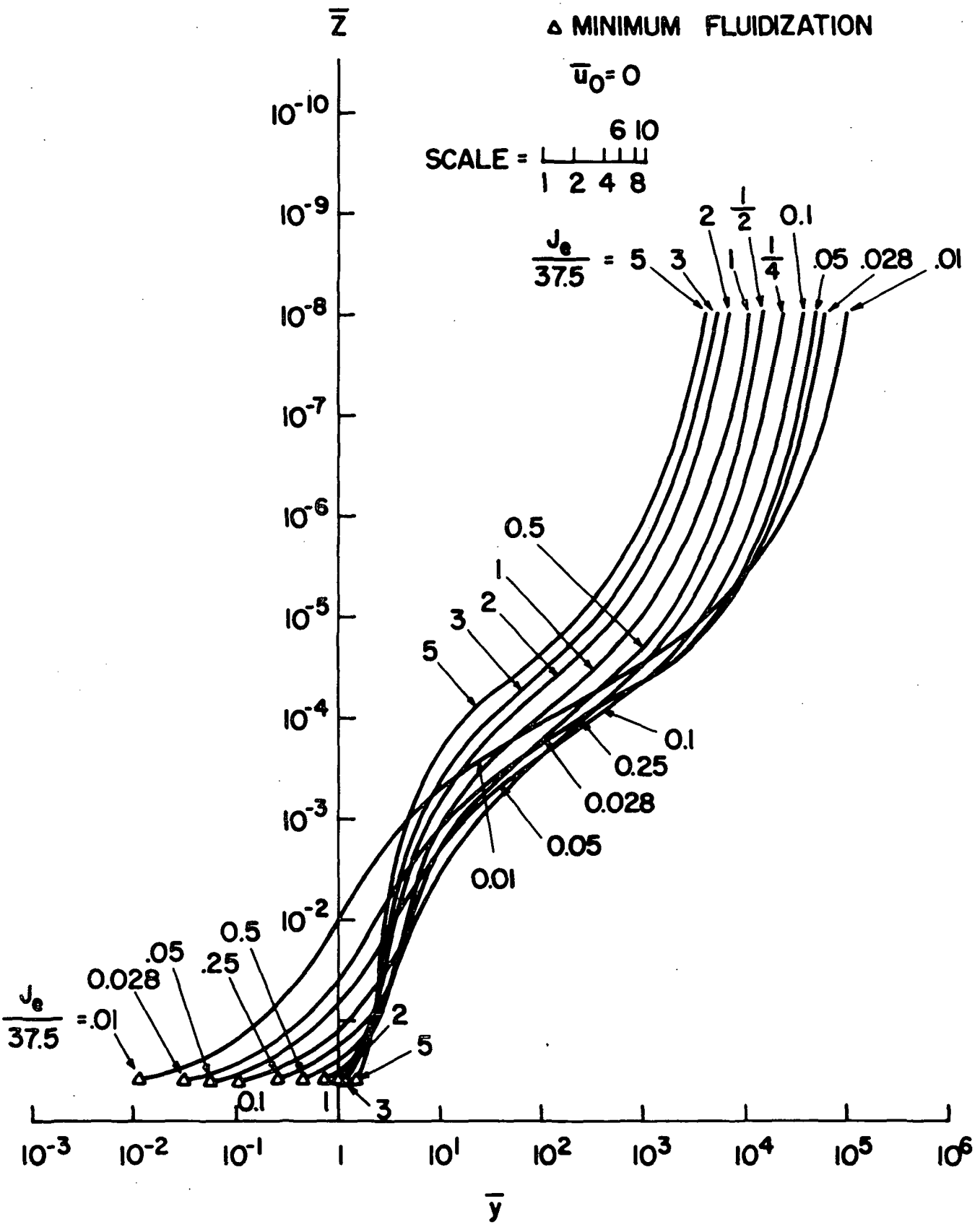

Fig. 8 Z AS A FUNCTION OF ALTITUDE

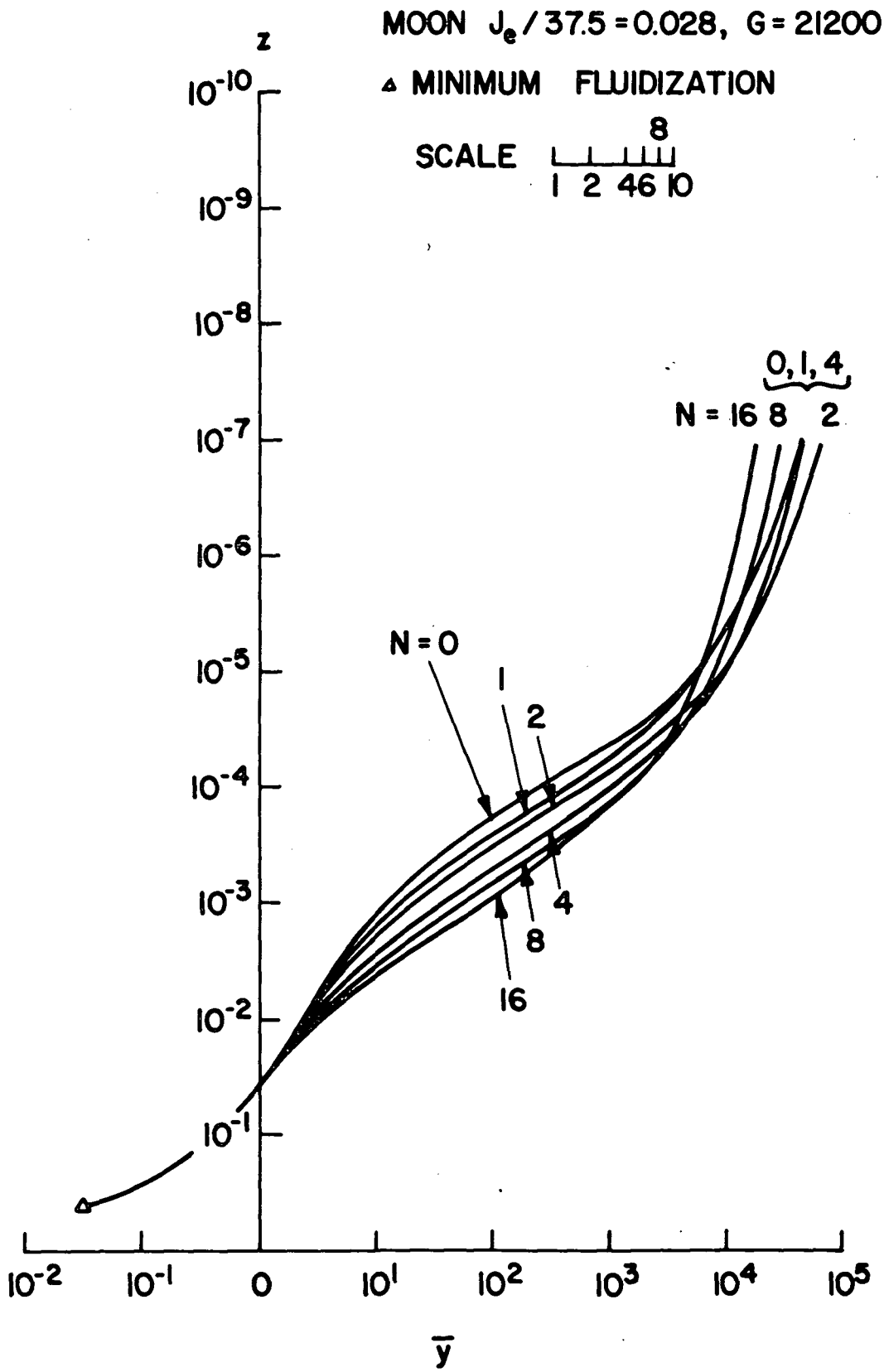

Fig. 9 Z AS A FUNCTION OF ALTITUDE FOR MOON, $\bar{u}_o = N/G$

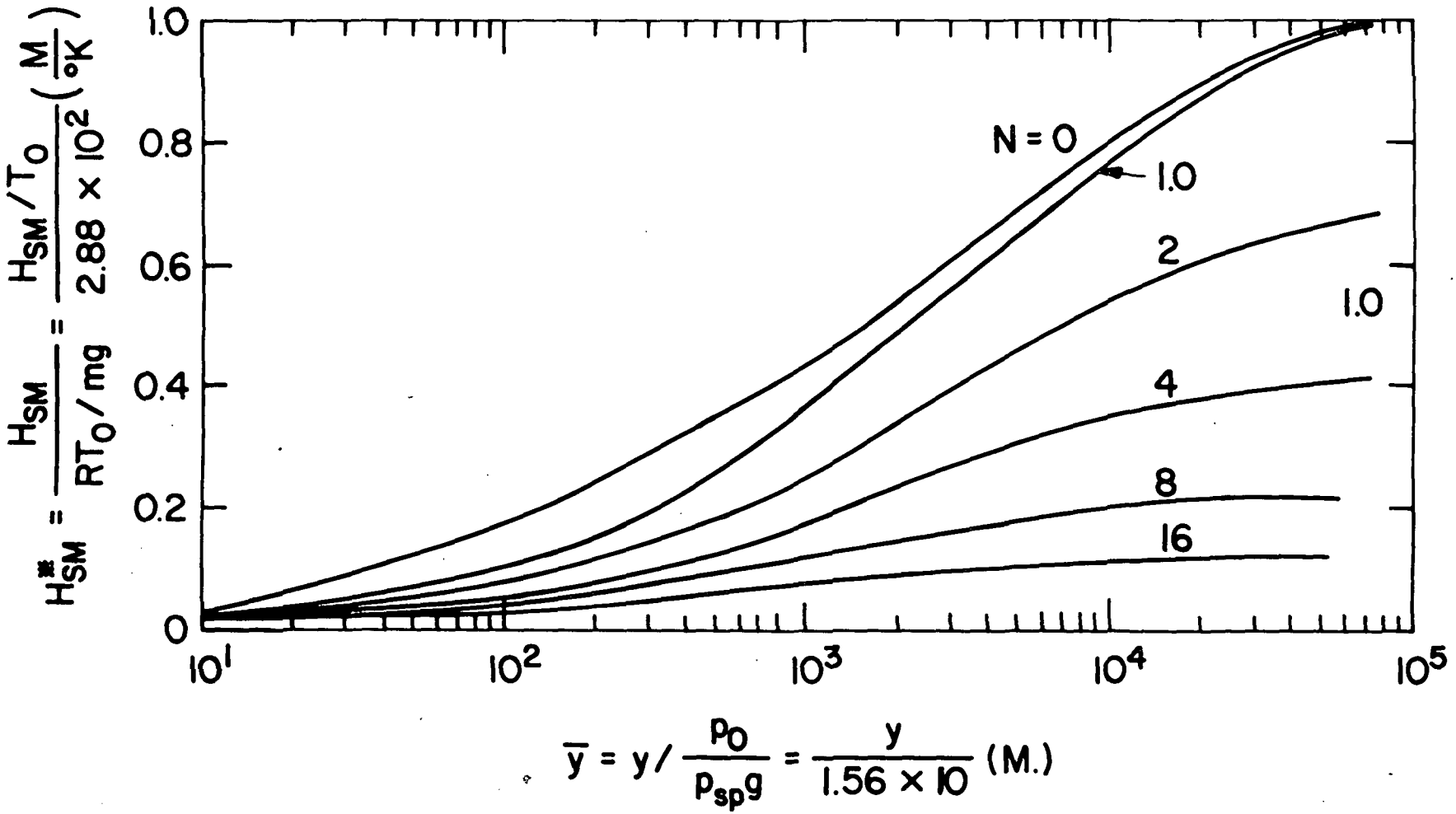

Fig. 10 SCALE HEIGHT AS A FUNCTION OF ALTITUDE

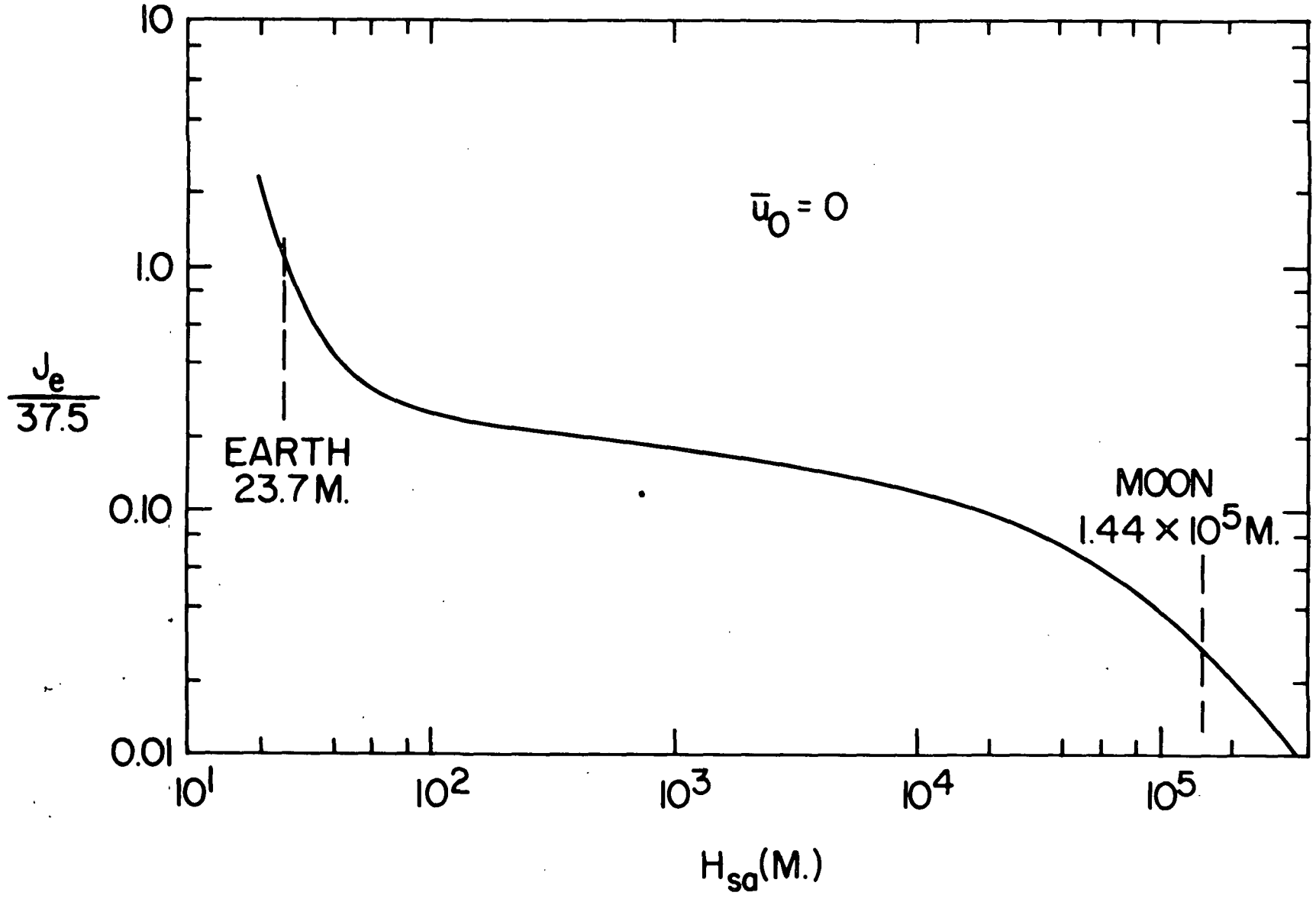

Fig. 11 AVERAGE SCALE HEIGHT AS A FUNCTION OF J_e

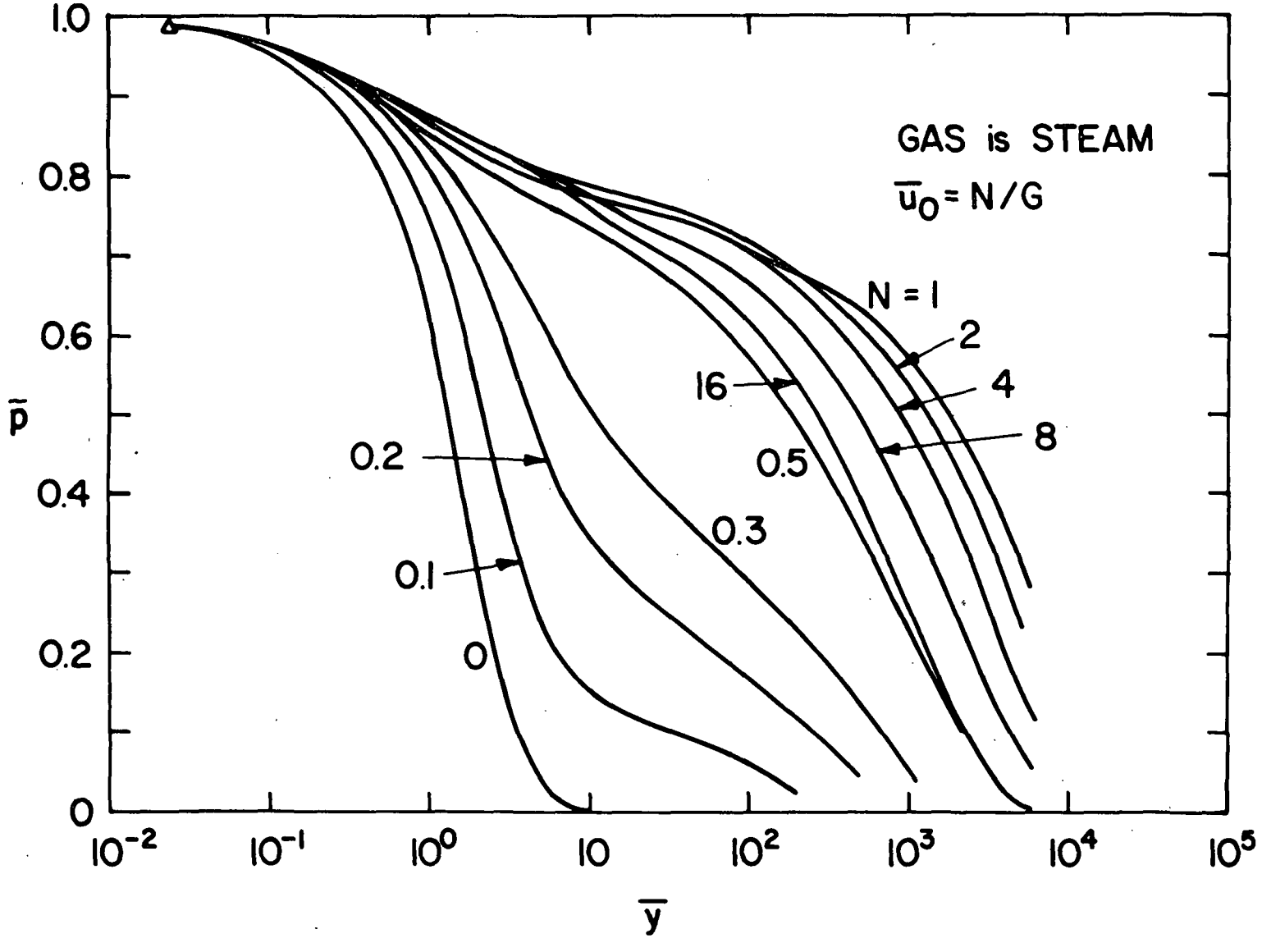

Fig. 12 $\bar{p}$ AS A FUNCTION OF ALTITUDE AT VARIOUS VALUES OF $\bar{u}_o$ ON MOON, $\bar{T} \neq 1$

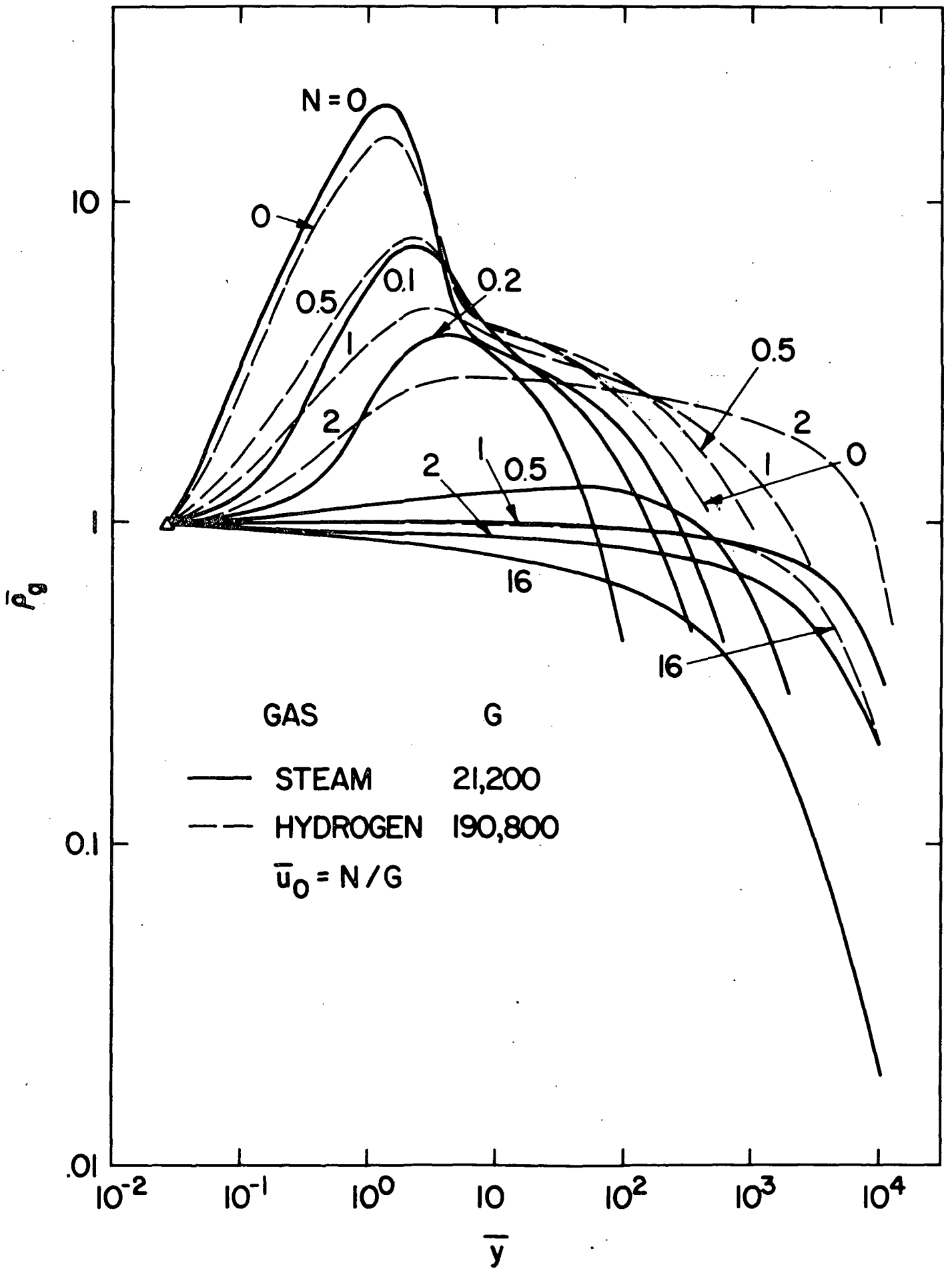

Fig. 13 $\bar{\rho}_g$ AS A FUNCTION OF ALTITUDE AT VARIOUS VALUES OF $\bar{u}_o$ ON MOON, $\bar{T} \neq 1$

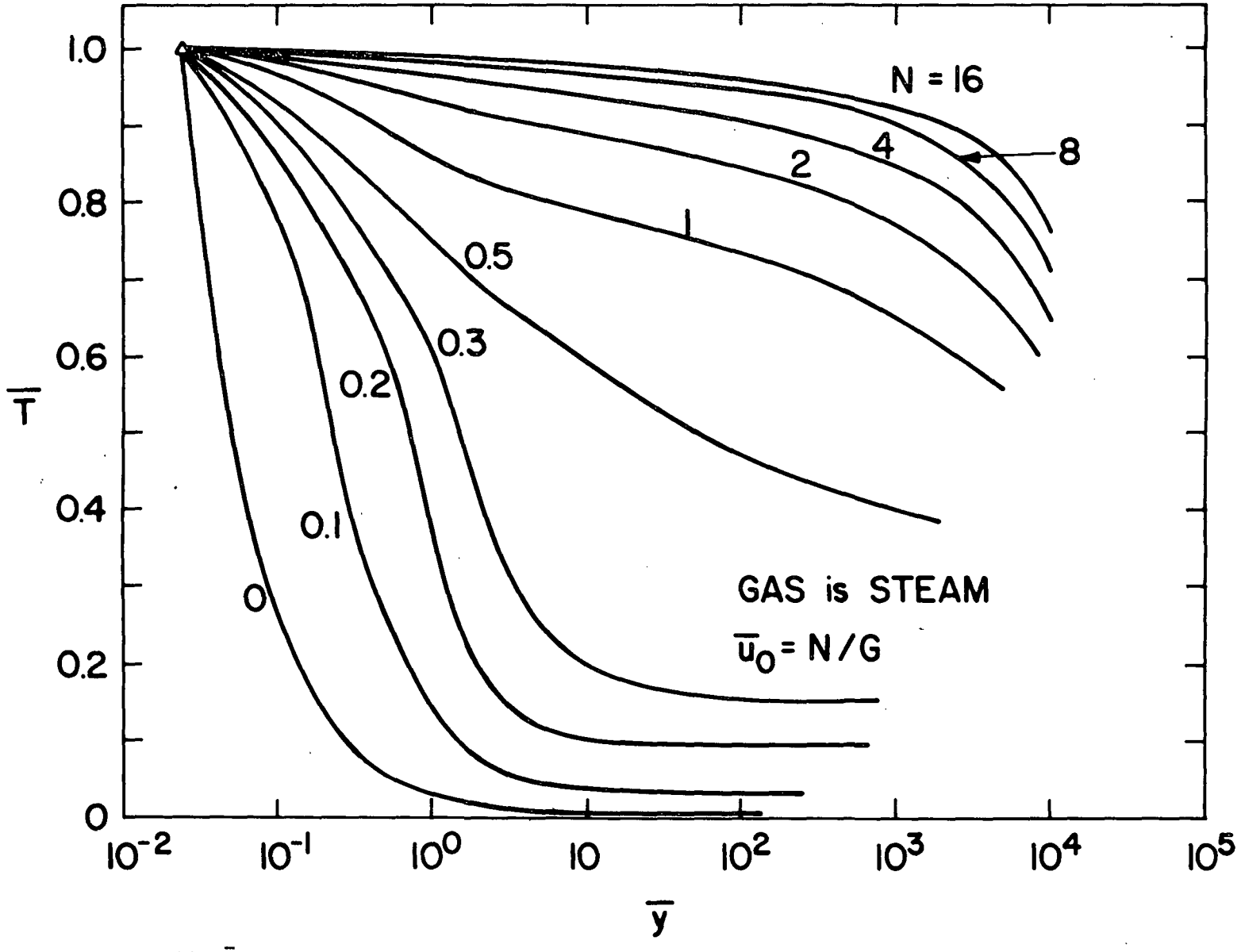

Fig. 14 $\bar{T}$ AS A FUNCTION OF ALTITUDE AT VARIOUS VALUES OF $\bar{u}_o$ ON MOON

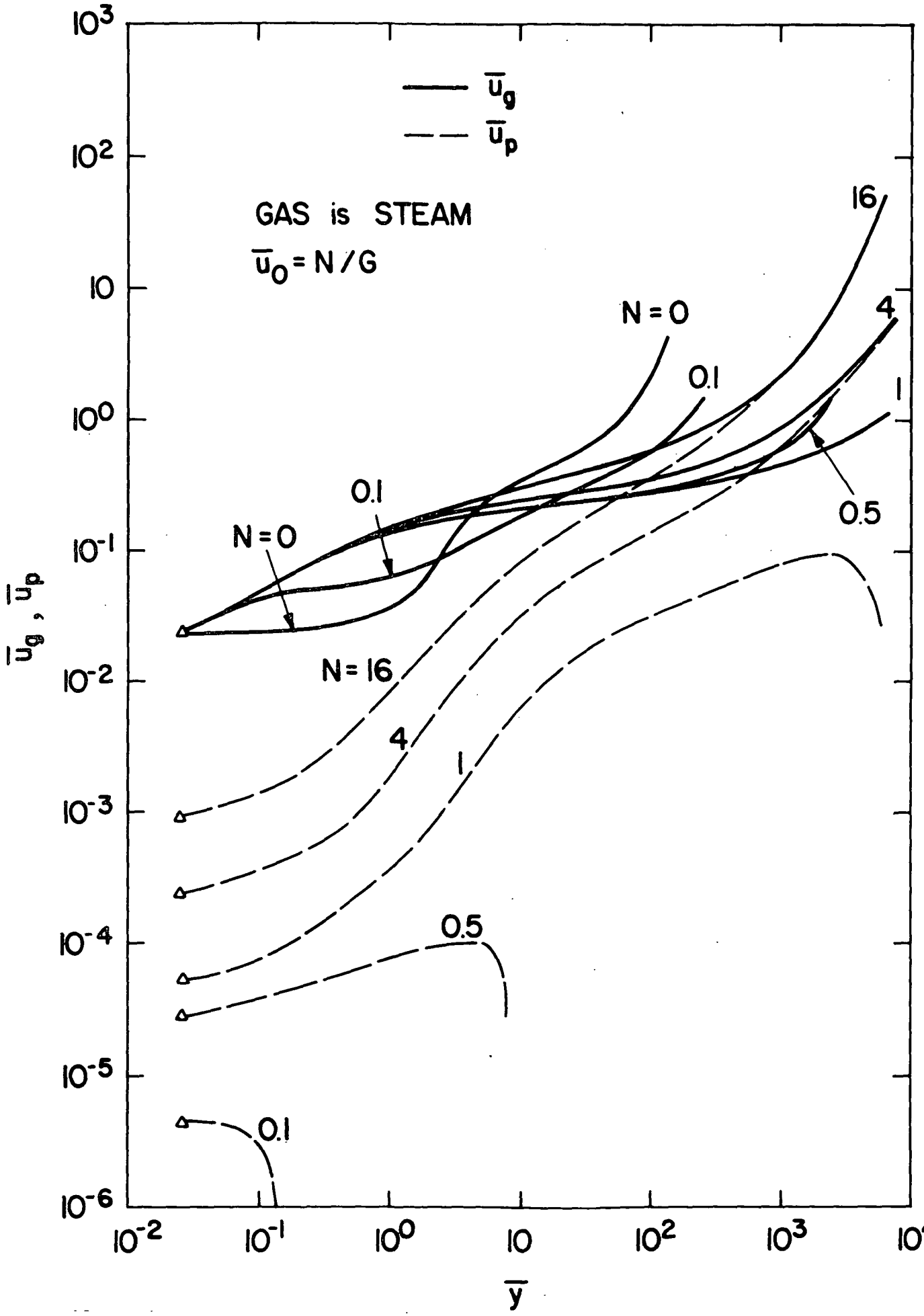

Fig. 15 $\bar{u}_g$ and $\bar{u}_p$ AS A FUNCTION OF ALTITUDE AT VARIOUS VALUES OF $\bar{u}_o$ ON MOON, $\bar{T} \neq 1$

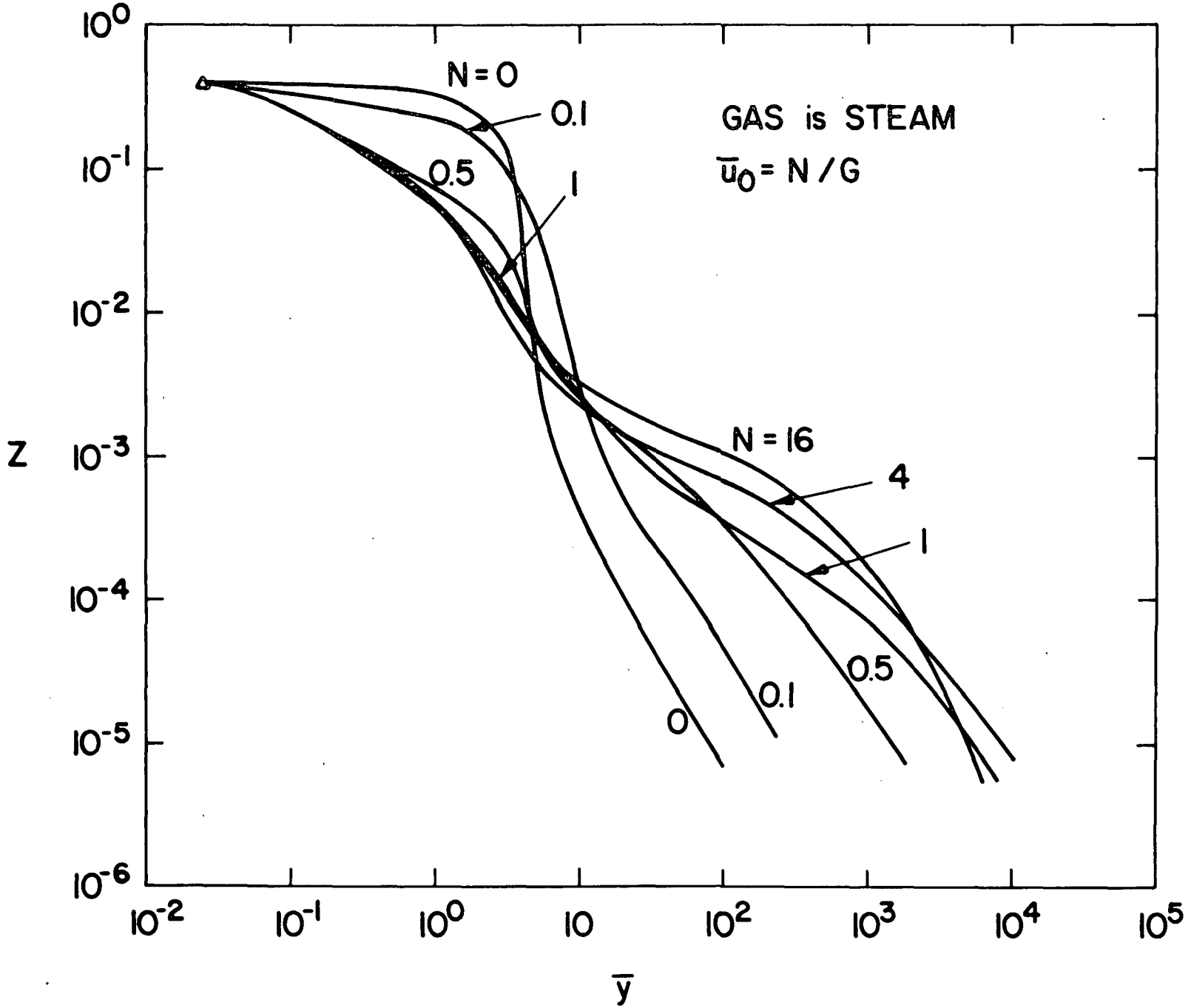

Fig. 16 Z AS A FUNCTION OF ALTITUDE AT VARIOUS VALUES OF $\bar{u}_o$ ON MOON

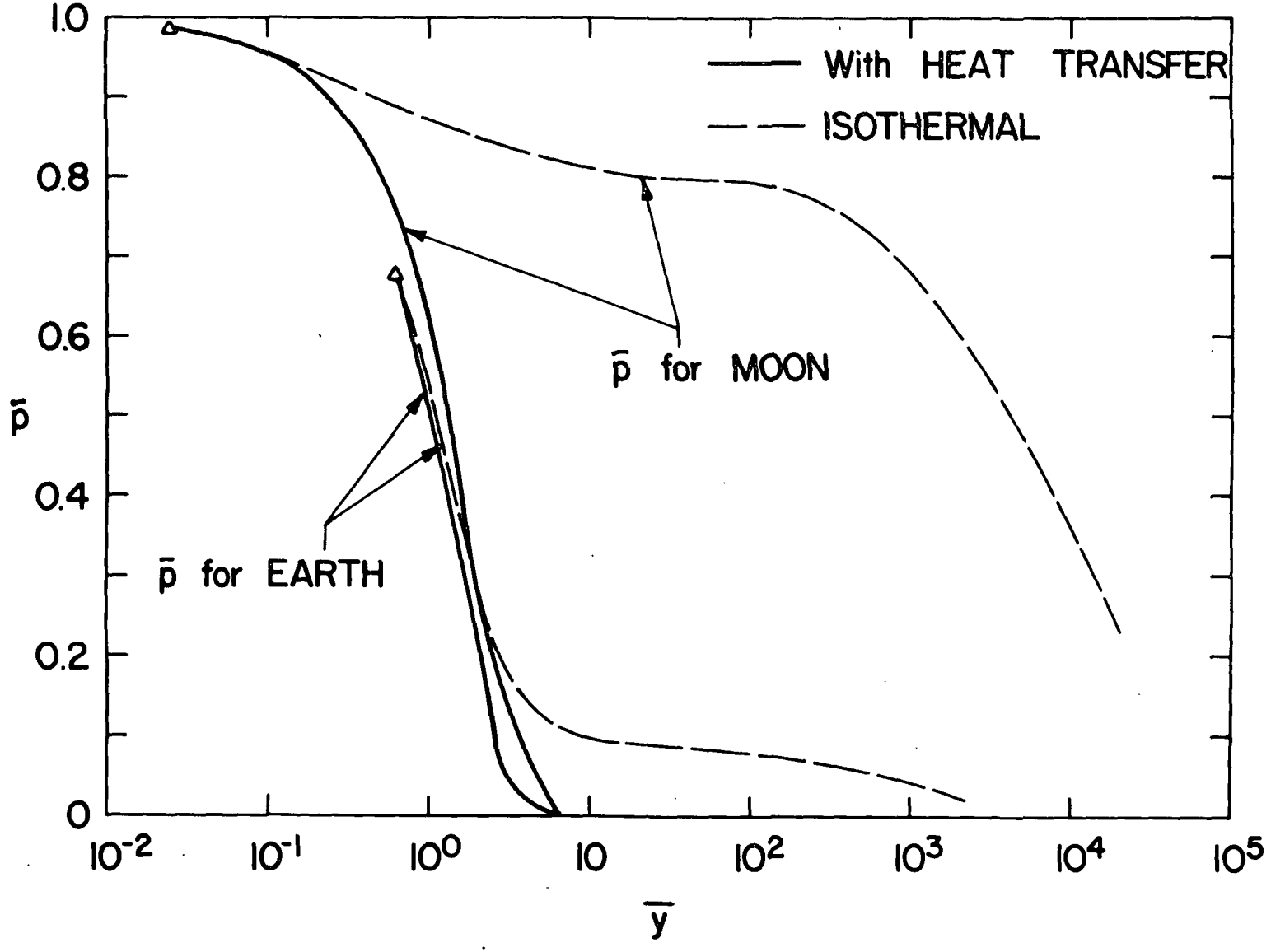

Fig. 17 COMPARISON OF $\bar{p}$ WITH AND WITHOUT HEAT TRANSFER AND ON MOON AND ON EARTH AT $\bar{u}_o = 0$

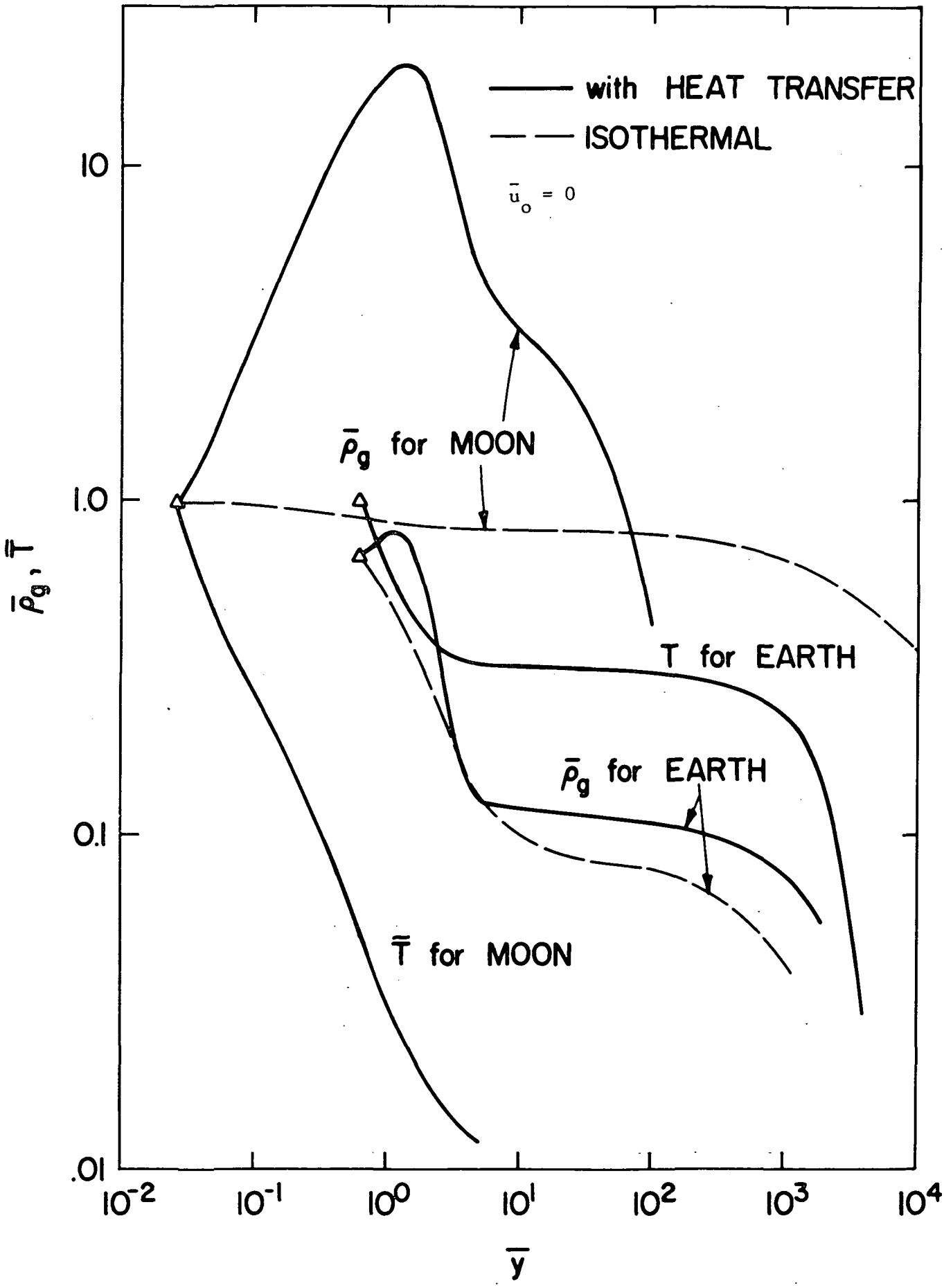

Fig. 18 COMPARISON OF $\bar{T}$ and $\bar{\rho}_g$ WITH AND WITHOUT HEAT TRANSFER AND ON MOON AND ON EARTH

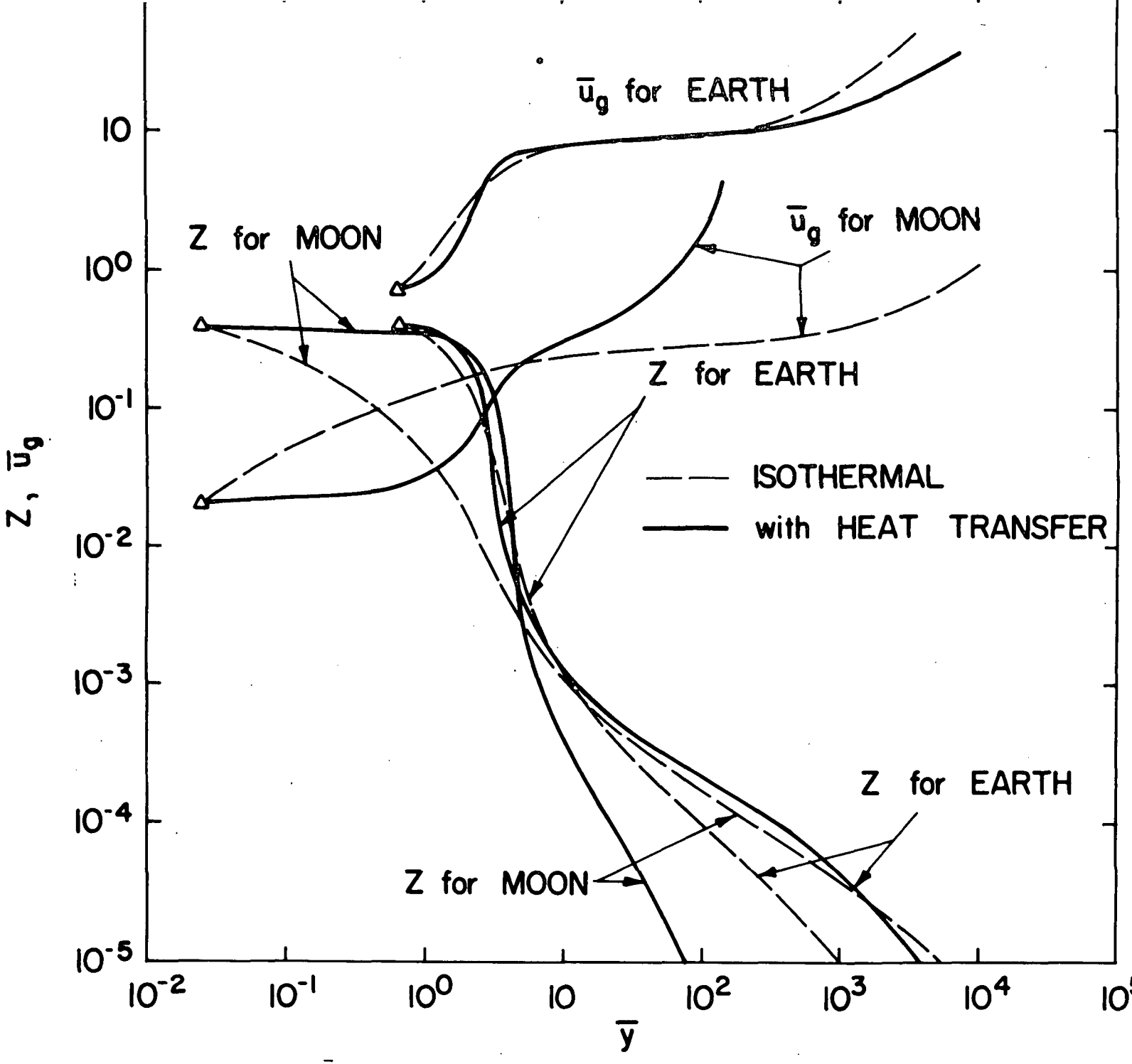

Fig. 19 COMPARISON OF $\bar{u}_g$ AND Z WITH AND WITHOUT HEAT TRANSFER AND ON MOON AND ON EARTH AT $\bar{u}_o = 0$

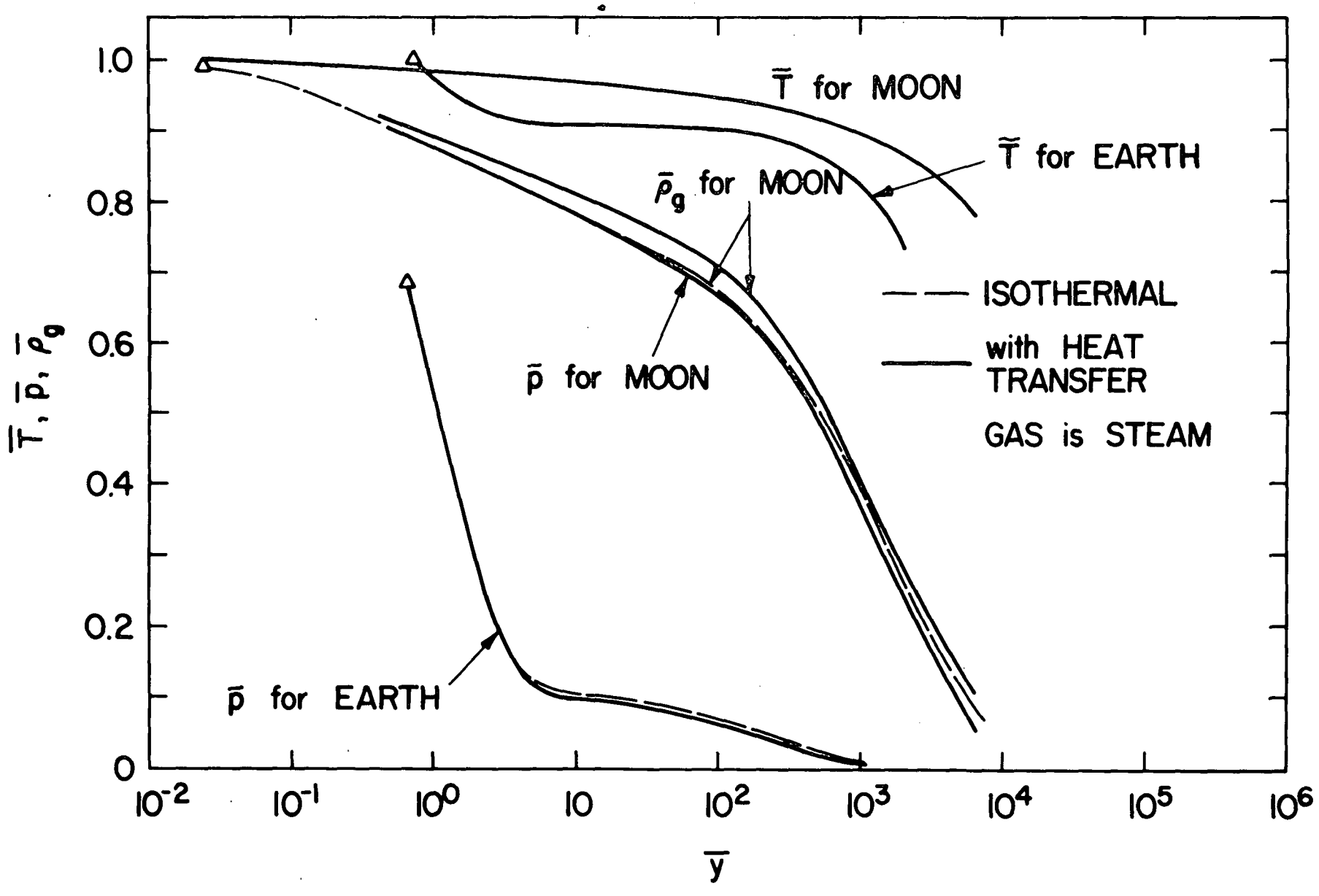

Fig. 20 COMPARISON OF $\bar{p}$, $\bar{\rho}_g$ AND $\bar{T}$ WITH AND WITHOUT HEAT TRANSFER AND ON MOON AND ON EARTH AT N = 8 ($\bar{u}_o$ = 8/G)

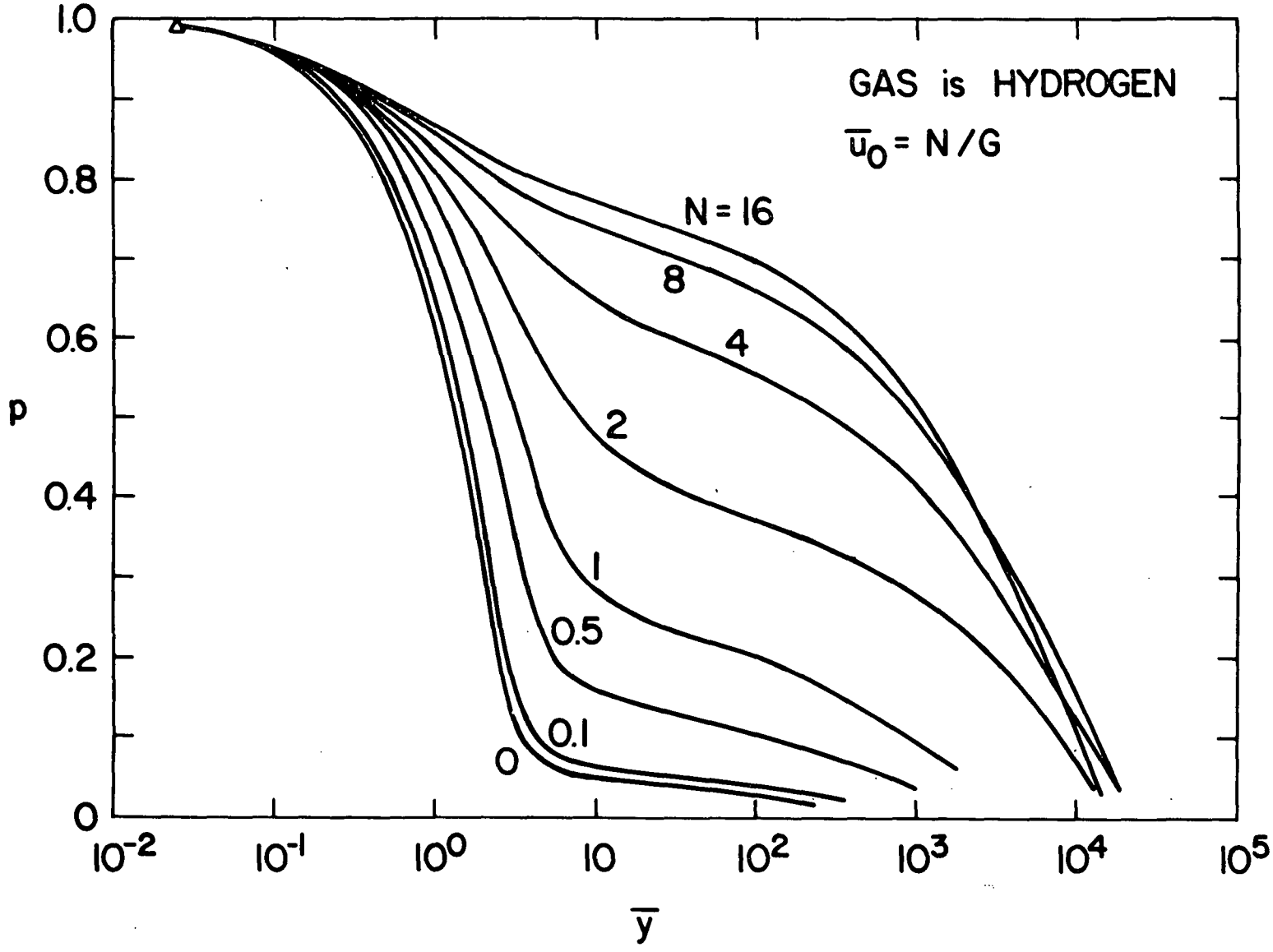

Fig. 21 $\bar{p}$ AS A FUNCTION OF ALTITUDE AT VARIOUS VALUES OF $\bar{u}_o$ ON MOON

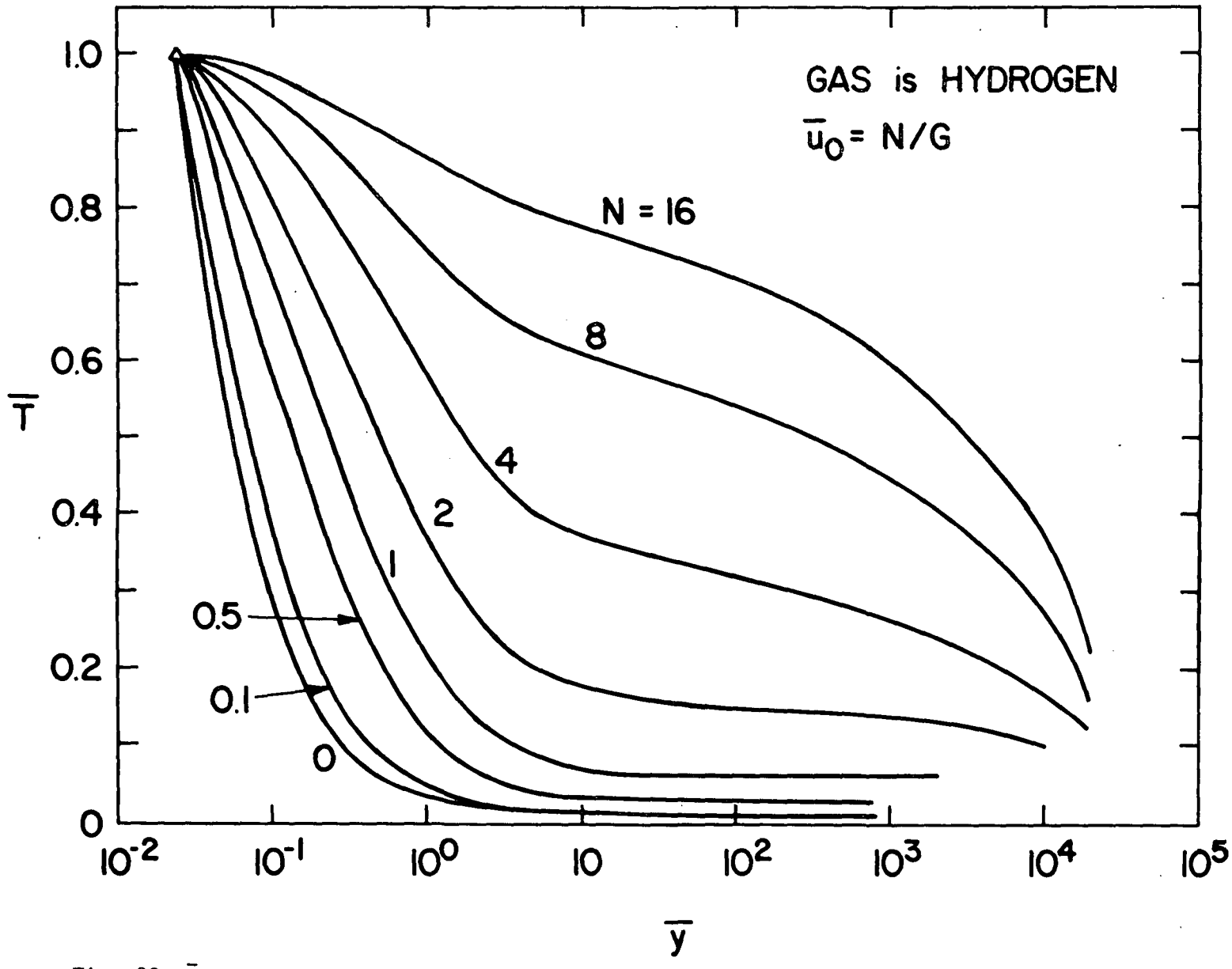

Fig. 22 $\bar{T}$ AS A FUNCTION OF ALTITUDE AT VARIOUS VALUES OF $\bar{u}_o$ ON MOON

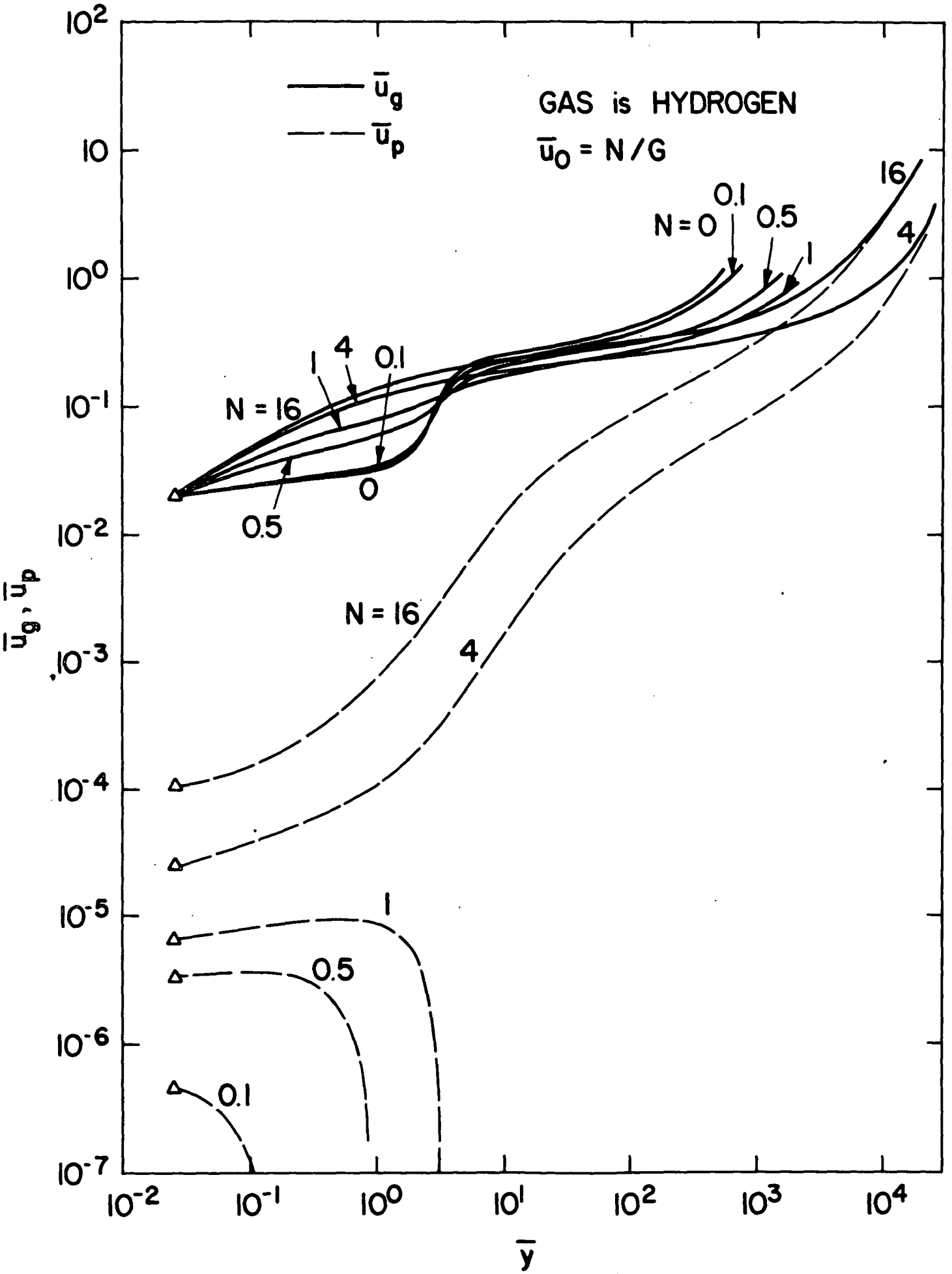

Fig. 23 $\bar{u}_g$ AND Z AS A FUNCTION OF ALTITUDE AT VARIOUS VALUES OF $\bar{u}_o$ ON MOON

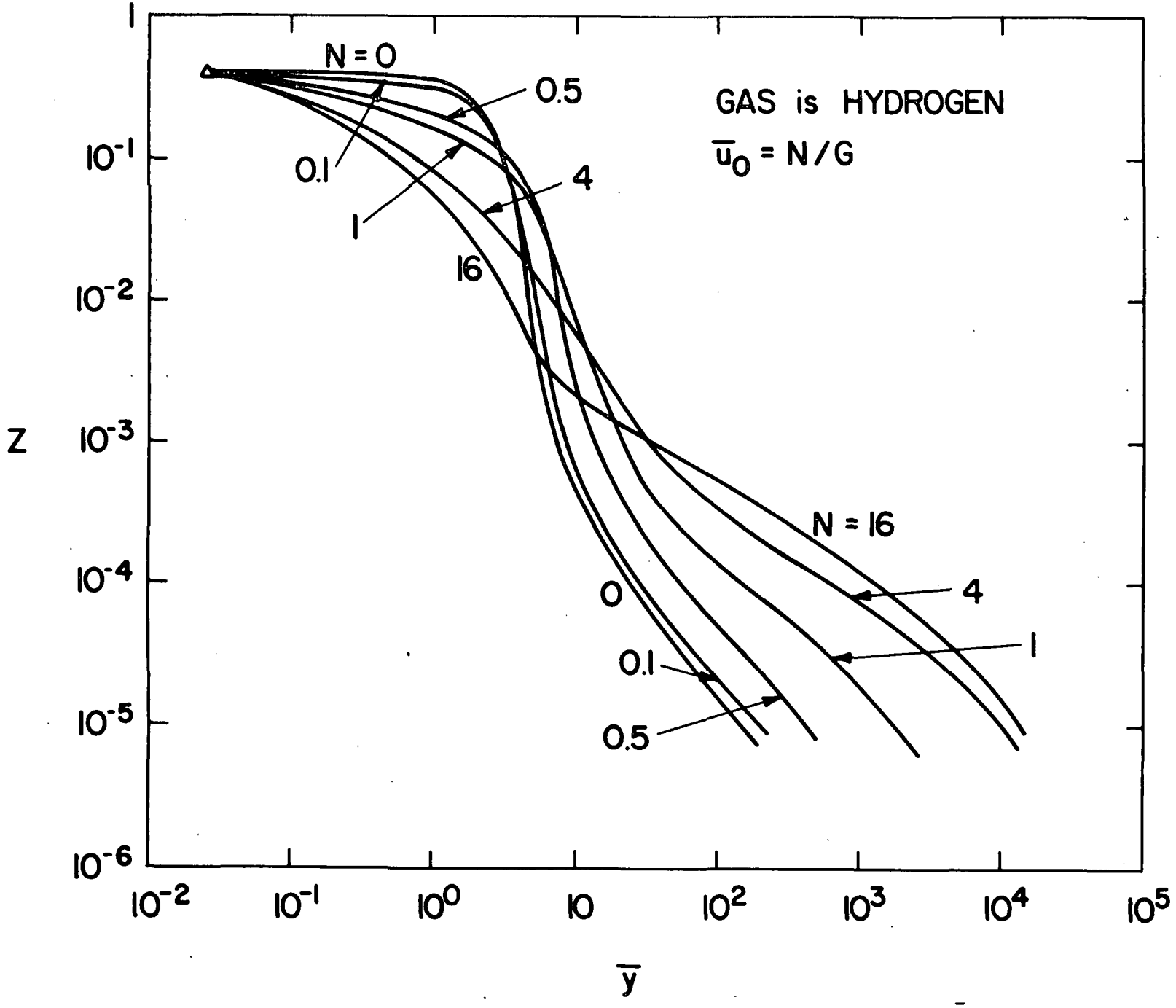

Fig. 24 Z AS A FUNCTION OF ALTITUDE AT VARIOUS VALUES OF $\bar{u}_o$ ON MOON

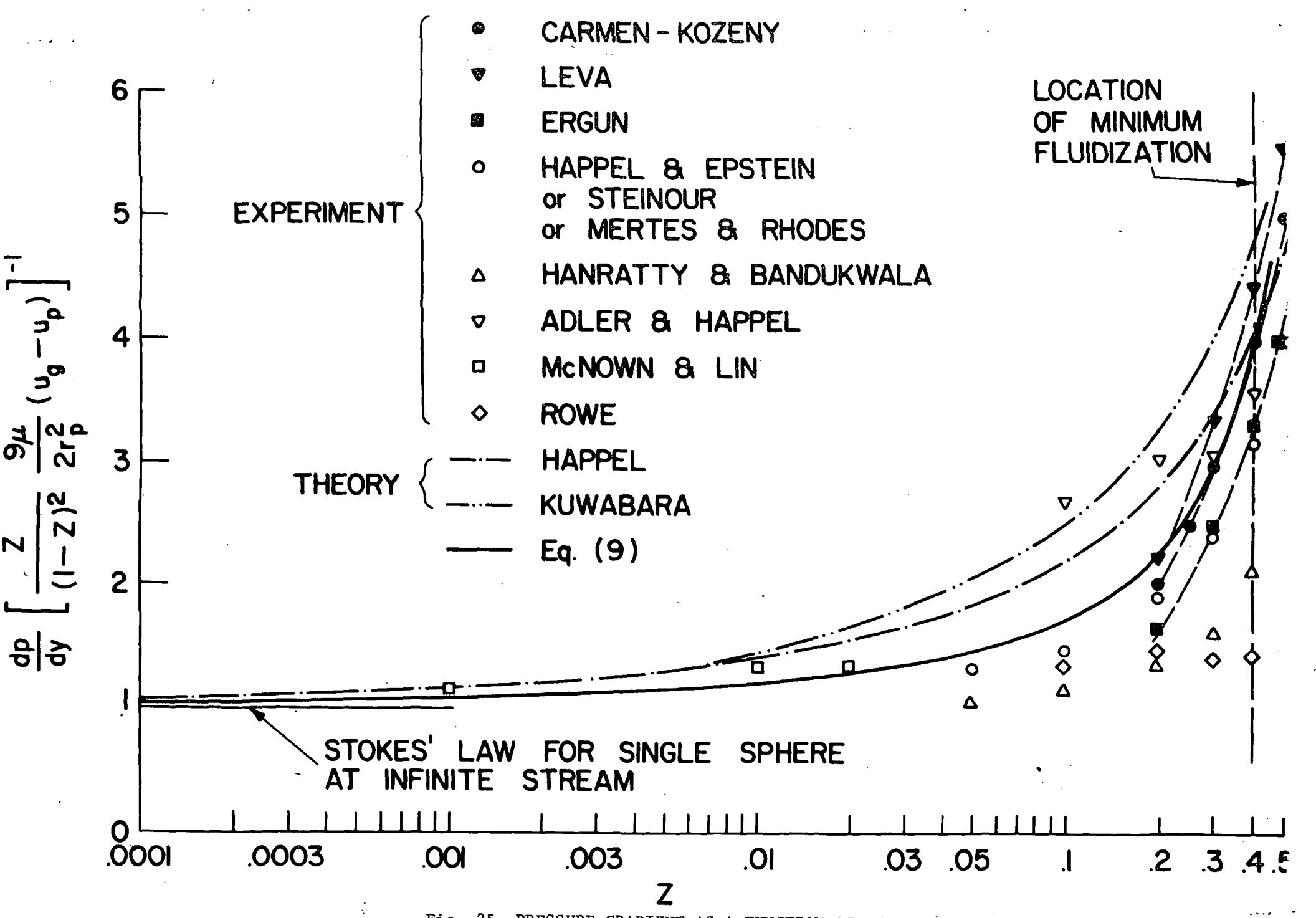

Fig. 25. PRESSURE GRADIENT AS A FUNCTION OF Z

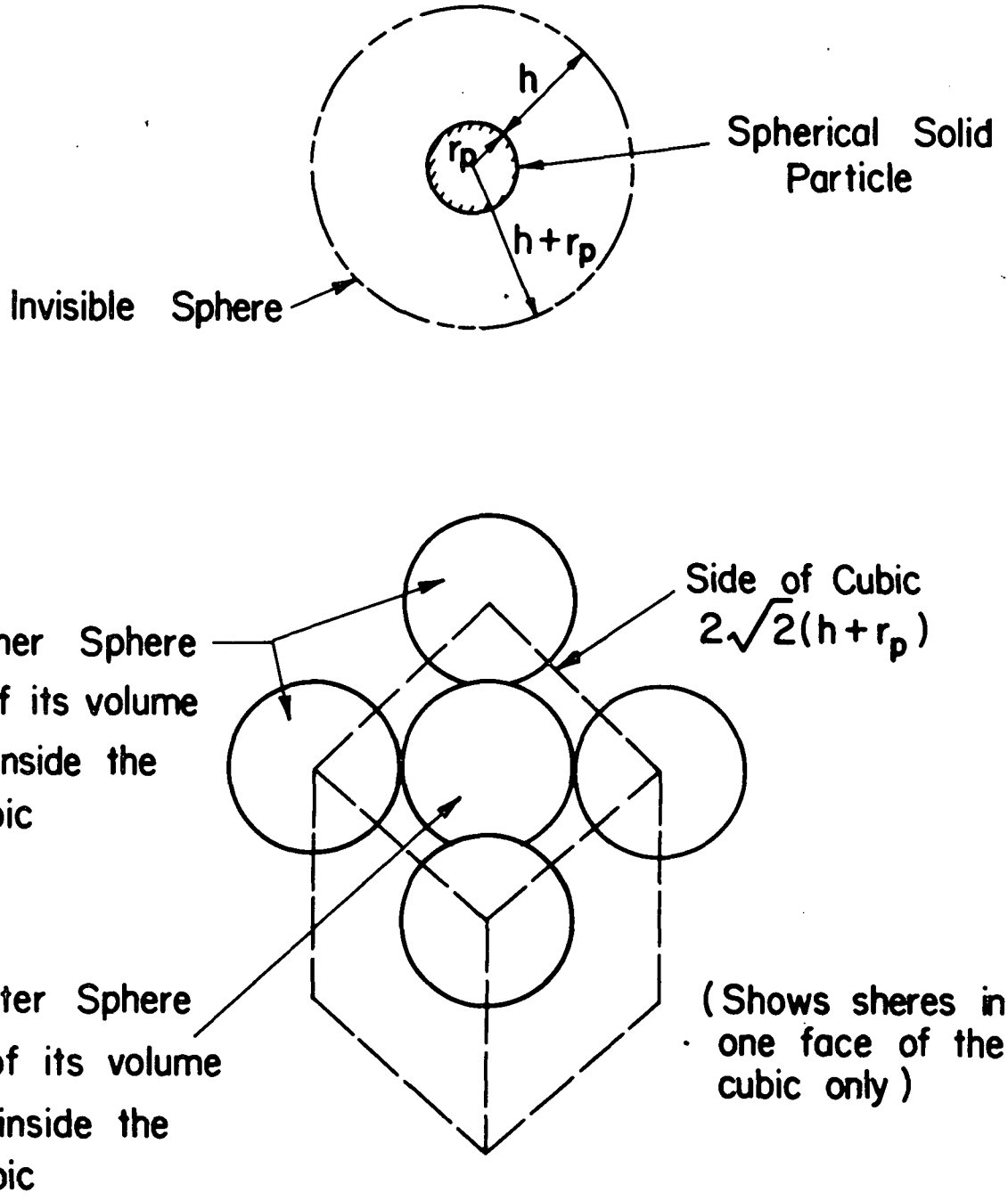

Fig. 26. GEOMETRY OF RHOMBOHEDRAL PACKING OF SPHERES